Acta Histochemica 115 (2013) 190–194

Contents lists available at SciVerse ScienceDirect

Acta Histochemica

journal homepage: www.elsevier.de/acthis

Short communication

Subtype-specific parafollicular localization of the neuropeptide manserin in the rat thyroid gland

Takeshi Ohkawara[a,*], Akiko Oyabu[a], Michiru Ida-Eto[a], Yasura Tashiro[a], Naoko Narita[b], Masaaki Narita[a]

[a] Department of Developmental and Regenerative Medicine, Mie University, Graduate School of Medicine, Mie, Japan
[b] Department of Education, Bunkyo University, Saitama, Japan

ARTICLE INFO

Article history:
Received 16 March 2012
Received in revised form 2 April 2012
Accepted 9 May 2012

Keywords:
Manserin
Thyroid gland
Parafollicular cell
Follicular epithelial cell
Neuropeptide
Chromogranin
Secretogranin

ABSTRACT

The thyroid gland is an endocrine organ which is involved in metabolism, neuroexcitability, body growth and development. The thyroid gland is also involved in the regulation of calcium metabolism, which is not yet fully understood. In this study, we investigated the localization of the granin-derived neuropeptide, manserin, in the adult rat thyroid gland. Manserin immunoreactivity was detected in thyroid follicular epithelial cells. Intense manserin signals were also detected in some, but not all, parafollicular cells, indicating that parafollicular manserin may be subtype-specific. These results indicate that thyroid manserin may play pivotal roles in parafollicular cells and follicular epithelial cells such as in calcium metabolism and/or thyroid hormone secretion.

Introduction

The thyroid gland plays an important role in the body by promoting metabolism, increasing neuroexcitability, accelerating body growth and development, and increasing cardiac function (Cheng et al., 2010). The thyroid gland is also involved in the regulation of calcium metabolism. A protein called thyroglobulin is secreted by thyroid follicular epithelial cells into the lumen of thyroid follicles. After iodination, thyroglobulin is again taken up by the follicular epithelial cells (Spitzweg et al., 2000). The hormones thyroxine (T4) and triiodothyronine (T3) are then released (internally secreted) into the circulation (Spitzweg et al., 2000).

Parafollicular cells of the thyroid gland are known to be involved in regulating serum Ca^{2+} levels through calcitonin secretion. Only one parafollicular cell type is known to date. However, the existence of somatostatin-positive and somatostatin-negative subtypes of parafollicular cells has been proposed (Sawicki and Zabel, 1997), suggesting that parafollicular cells may be heterogeneous. However, the precise morphological and functional distinctions among parafollicular cells have still not been elucidated.

We recently isolated manserin, a neuropeptide composed of 40 amino acids, by combining HPLC and affinity purification (Yajima et al., 2004). Manserin is distributed in the rat pituitary, hypothalamic nuclei, adrenal gland, duodenum epithelial cells, cerebellum, inner ear, and β and δ cells in the pancreatic islets (Yajima et al., 2004, 2008; Kamada et al., 2010; Tano et al., 2010; Ohkawara et al., 2011; Ida-Eto et al., 2012), indicating that manserin plays roles in several endocrine systems. Manserin has not previously been found in the thyroid gland. However, the fact that SgII, a manserin precursor, occurs in thyroid parafollicular cells (Weiler et al., 1989; Schmid et al., 1992) suggests that manserin might also occur in the thyroid gland. Because SgII is reported to have Ca^{2+}-binding ability (Yoo et al., 2007), manserin is also expected to have some roles in Ca^{2+} metabolism. In addition, parafollicular cells secrete numerous regulatory peptides that play important roles in their functions (Sawicki, 1995). For these reasons, we sought to identify the localization of manserin in the adult thyroid gland.

Materials and methods

Animals

Four male Wistar rats (8–12 weeks old) were used. All animal experiments were approved by the Committee of Laboratory Animal Research Center at Mie University.

* Corresponding author at: Department of Developmental and Regenerative Medicine, Mie University, Graduate School of Medicine, 2-174 Edobashi, Tsu, Mie 514-8507, Japan.
E-mail address: tohkawara@doc.medic.mie-u.ac.jp (T. Ohkawara).

0065-1281/$ – see front matter © 2012 Elsevier GmbH. All rights reserved.
http://dx.doi.org/10.1016/j.acthis.2012.05.003

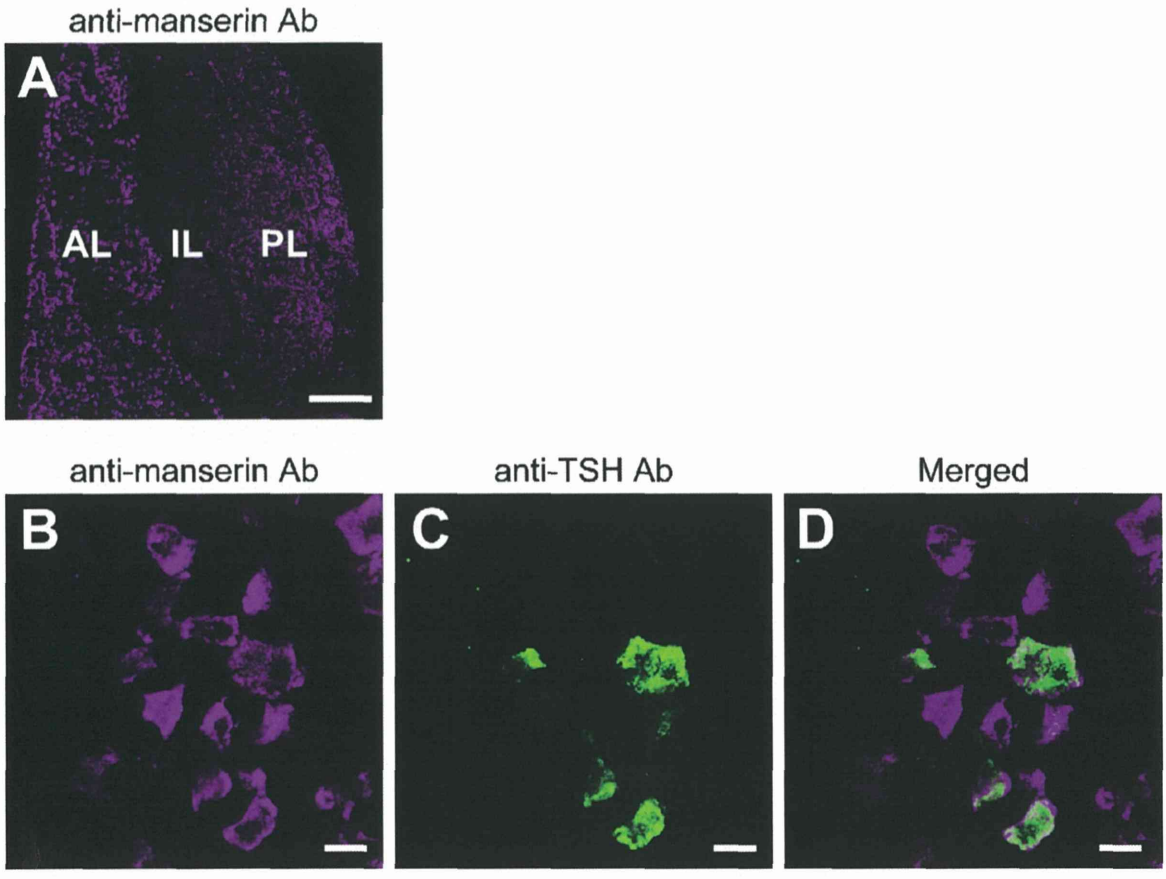

Fig. 1. Localization of manserin in TSH-expressing cells in the rat pituitary gland. Antigen–antibody complexes were detected by immunofluorescent staining (A–D). Manserin signals were detected in the anterior, intermediate, and posterior lobes of the pituitary gland (A). Double immunostaining with anti-manserin antibody (B) and anti-TSH antibody (C) was also shown. (D) is a merged image. AL, anterior lobe; IL, intermediate lobe; PL, posterior lobe. Scale bars = 200 μm (A) and 10 μm (B–D).

Tissue preparation

Anesthetized rats were transcardially perfused with 0.9% saline followed by perfusion with 4% paraformaldehyde (PFA) in phosphate buffered saline (PBS) (Tano et al., 2010). The thyroid and pituitary glands were dissected and immersed in 4.0% PFA in PBS overnight at 4 °C. For cryosectioning, the pituitary gland was cryoprotected in 30% sucrose, embedded in O.C.T. compound (Sakura Finetek, Tokyo, Japan), and sectioned at 9 μm thickness on a Leica CM1850 cryostat (Leica Microsystems, Wetzlar, Germany). For paraffin sectioning, the thyroid gland was immersed in a graded ethanol series and xylene and embedded in paraffin followed by sectioning at 7 μm using a rotary microtome.

Anti-manserin antibody

Affinity-purified rabbit anti-manserin antibody was prepared as described previously (Kamada et al., 2010). The specificity of the antibody was confirmed by immunoblotting (Yajima et al., 2004) and a preabsorption test.

Immunostaining

The thyroid and pituitary glands were immunostained as described previously (Yajima et al., 2004, 2008). In brief, sections were incubated in 3.0% H_2O_2 in PBS, washed with PBS, and blocked with 10% fetal bovine serum (FBS) in PBS containing 0.1% Triton X-100 for 1 h. The sections were then labeled with rabbit anti-manserin antibody overnight at 4 °C, incubated with biotin-conjugated anti-rabbit IgG (Chemicon, CA, USA), and washed with PBS. The sections were then stained by the ABC method and visualized with 3,3′-diaminobenzidine (DAB) using the Vectastain Elite ABC Kit (Vector Laboratories, Burlinghame, CA, USA). For counterstaining, sections of the thyroid gland were stained with Mayer's hematoxylin solution (Wako Pure Chemicals, Osaka, Japan).

Frozen sections of the pituitary gland were immunofluorescently stained as described previously (Ohkawara et al., 2004; Tano et al., 2010). For single immunostaining, the sections were incubated with anti-manserin antibody (Kamada et al., 2010) at 4 °C overnight. For double immunostaining, the sections were incubated with rabbit anti-manserin antibody (Kamada et al., 2010) and goat anti-thyroid-stimulating hormone (TSH) β chain antibody (Santa Cruz Biotechnology Inc., Santa Cruz, CA, USA) overnight at 4 °C, followed by incubation with fluorescently labeled secondary antibodies. Concentrations of secondary antibodies used in this study were as follows: Alexa 488-conjugated donkey anti-goat IgG (2 μg/ml; Invitrogen, Carlsbad, CA, USA) and Alexa 568-conjugated donkey anti-rabbit IgG (2 μg/ml; Invitrogen).

Paraffin sections of the thyroid gland were deparaffinized and rehydrated through a graded ethanol series. After rehydration, the sections were treated with citrate buffer (pH 6.0) for target retrieval, followed by blocking with 10% FBS in PBS containing 0.1% Triton X-100 for 1 h. The sections were then incubated with primary antibodies at 4 °C overnight, followed by incubation with fluorescently labeled secondary antibodies. Primary antibodies used for immunostaining of the paraffin sections were as follows: rabbit anti-manserin antibody (Kamada et al., 2010), rabbit anti-SgII antibody (QED Bioscience, San Diego, CA, USA), and goat anti-calcitonin antibody (Santa Cruz Biotechnology Inc.).

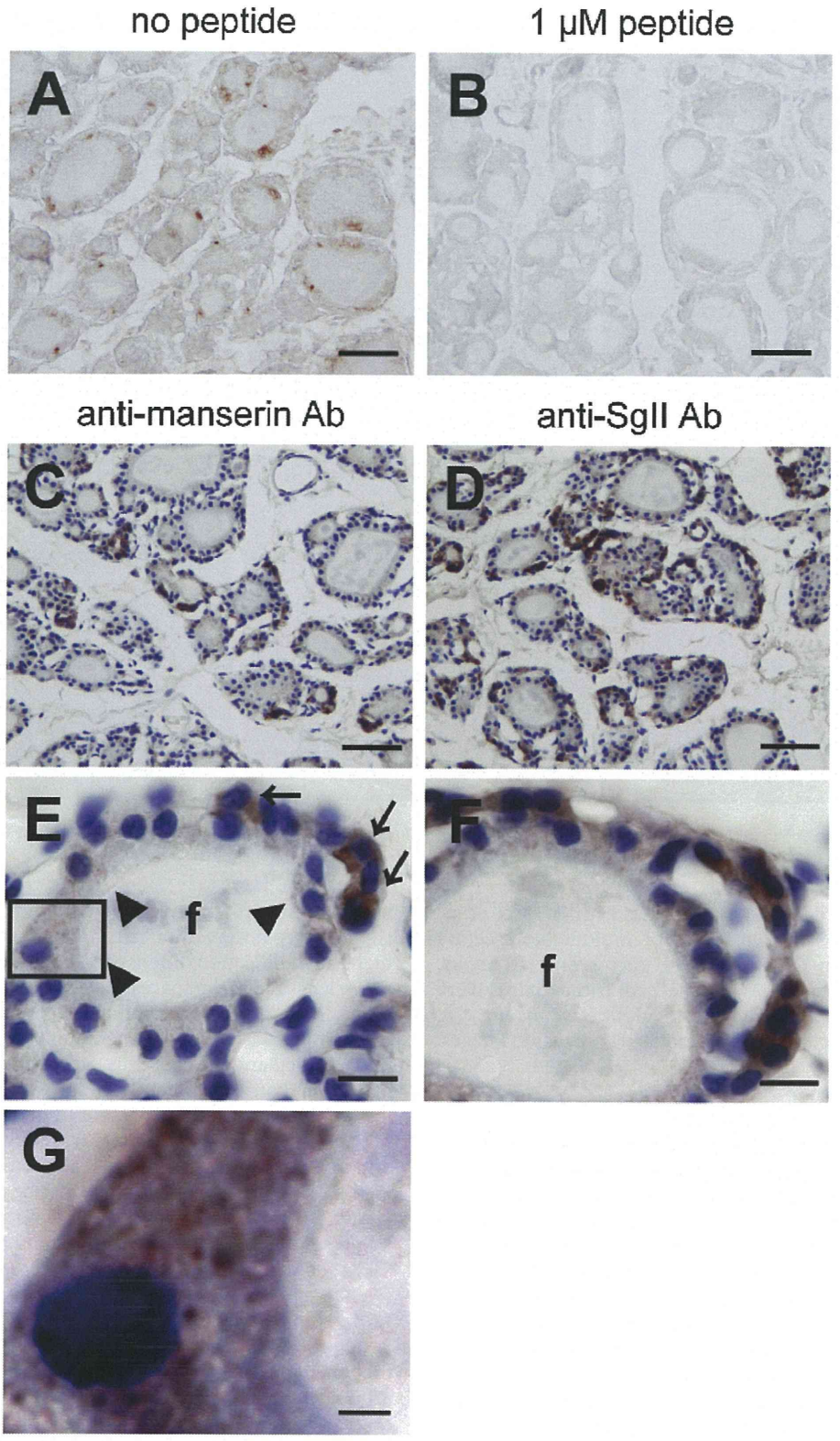

Fig. 2. Distribution of manserin in the thyroid gland. Antigen–antibody complexes were detected by DAB staining (*brown*, A–G). The specificity of anti-manserin antibody was confirmed by the preabsorption test. In the preabsorption test, manserin signals were detected when anti-manserin antibody was incubated with PBS (A), but no signal was detected when anti-manserin antibody was preabsorbed with a recombinant peptide (10^{-6} M) (B). In the thyroid gland, manserin signals (C, E and G) and SgII signals (D and F) were detected. *Arrows* in (E) indicate localization of manserin in the cells located in the interfollicular space. *Arrowheads* in (E) indicate localization of manserin in the follicular epithelial cells. (G) shows higher magnification view of the boxed area in (E). In (C)–(G), nuclei were counterstained with Mayer's hematoxylin solution. f, follicle. Scale bars = 50 μm (A–D), 10 μm (E and F) and 2 μm (G). (For interpretation of the references to color in this figure legend, the reader is referred to the web version of the article.)

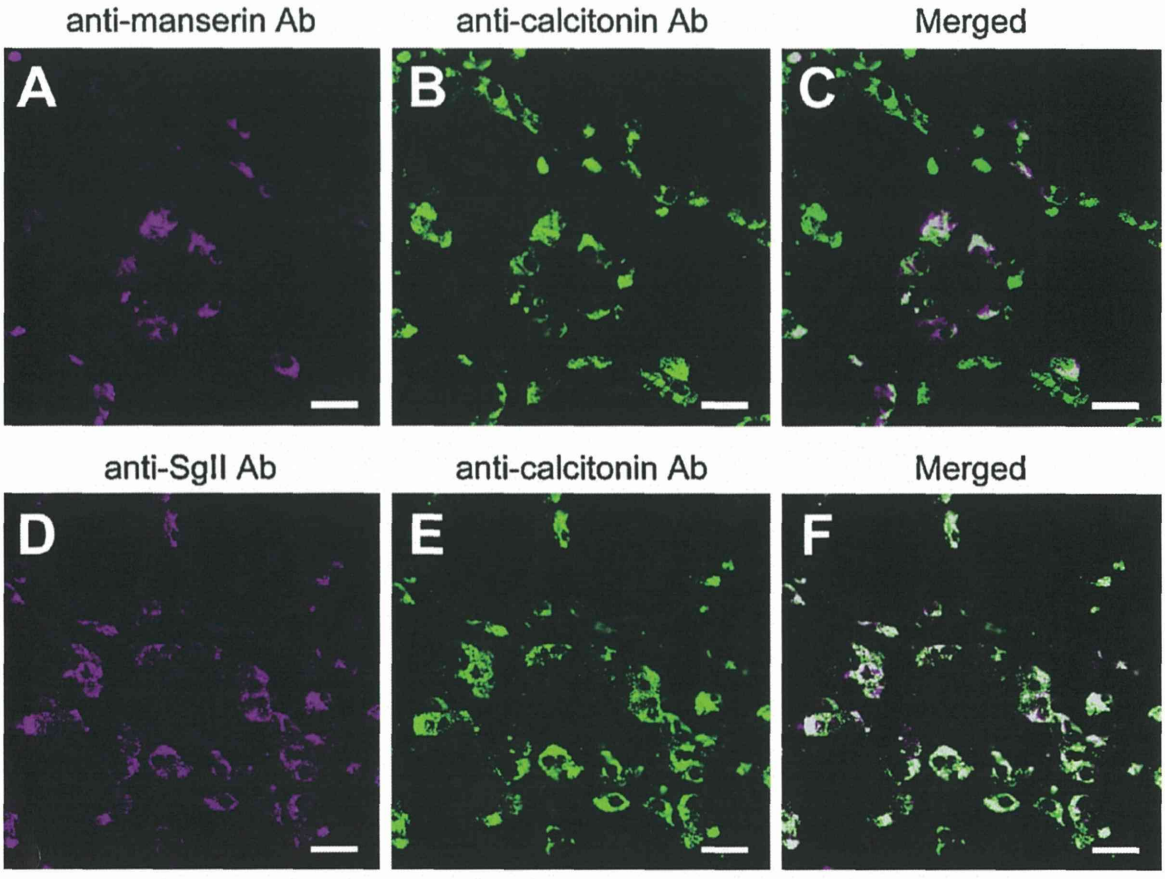

Fig. 3. Distribution of manserin or SgII in the parafollicular cells. Double immunostaining was performed with anti-calcitonin antibody (B and E) and anti-manserin (A) or anti-SgII antibody (D). Merged images are also shown (C and F). Scale bar = 20 μm (A–F).

Signals were visualized using an Olympus FV1000 laser scanning microscope (Olympus, Tokyo, Japan) for immunofluorescently stained sections and an Olympus BX50 microscope (Olympus, Japan) for sections stained by the ABC method. These images were processed using Adobe Photoshop CS5.1 (Adobe Systems Inc., CA, USA). Immunoreactive cells were counted using processed images.

Results

Because blood levels of thyroid hormones are controlled by TSH produced in the pituitary gland, we examined whether manserin was present in TSH-expressing cells in the rat pituitary gland. Manserin was detected in the anterior, intermediate, and posterior lobes of the pituitary gland (Fig. 1A). In our previous study, manserin was not localized in the intermediate and posterior lobes (Yajima et al., 2004). This apparent discrepancy may be explained because of (1) DAB staining, which is less sensitive than immunofluorescent staining and (2) anti-serum, but not affinity-purified anti-manserin antibody was used. Double staining with anti-manserin antibody and anti-TSH antibody revealed that manserin was present in TSH-expressing cells (Fig. 1B–D). The TSH-expressing cells were exclusively manserin positive, whereas only some manserin-positive cells were TSH positive (30.5% of 246 manserin-positive cells counted). Since manserin was colocalized with follicle stimulating hormone (FSH)-expressing cells (Yajima et al., 2004), cells that are manserin-positive and TSH-negative are thought to be FSH-expressing cells. These results indicate that manserin is present in TSH-expressing cells in the rat pituitary gland.

Because manserin is colocalized with the TSH-expressing cells in the pituitary gland as described above, the peptide is assumed to be localized in the thyroid gland. Intense, but scattered, manserin signals were observed in cells around follicles (Fig. 2A and C). At higher magnification, intense manserin-positive cells were exclusively localized in the space between follicles, i.e., the interfollicular space, suggestive of parafollicular cells (Fig. 2E, arrows). Under careful observation, manserin immunoreactivity was also observed in the follicular epithelial cells, although the immunostaining was less faint than parafollicular cells (Fig. 2E and G). These results indicate that manserin is present in follicular epithelial as well as in parafollicular cells. No signal was detected when the manserin antibody was preabsorbed with a recombinant peptide (10^{-6} M; Fig. 2B) and when the primary antibody was omitted (data not shown). SgII, a precursor of manserin that has been reported to be present in the thyroid gland (Schmid et al., 1992; Weiler et al., 1989), showed a staining profile quite similar to that of manserin (Fig. 2D and F).

To confirm the presence of manserin in parafollicular cells, we tested the colocalization of manserin with calcitonin, a parafollicular hormone that regulates blood Ca^{2+} levels. As reported (Foster, 1968), anti-calcitonin antibody stains almost all parafollicular cells (Fig. 3B and E). However, only 35.8% of 447 calcitonin-expressing cells counted were manserin positive (Fig. 3A and C), suggesting the existence of distinct forms of parafollicular cells. On the other hand, almost all (96.4%) of the calcitonin-expressing cells counted were SgII positive (Fig. 3D and F). These results suggest that manserin may localize only in a specific subtype of the parafollicular cells.

Discussion

This is the first study to demonstrate the presence of manserin in thyroid follicular epithelial cells and also in parafollicular cells.

This result suggests that thyroid manserin may play some roles in the thyroid functions such as Ca^{2+} metabolism and hormone secretion.

We detected manserin signals as fine puncta in the cytoplasm of thyroid follicular epithelial cells. Because thyroid hormones are produced by the proteolytic cleavage of iodinated thyroglobulin in lysosomes and released by follicular epithelial cells into the blood, the punctate signals of manserin in the follicular epithelial cells indicate that manserin may reside in the lysosome where thyroid hormones were produced. Granin family proteins play a role in the formation of secretory vesicles (Iacangelo and Eiden, 1995; Kim et al., 2001), and there is evidence that the SgII-derived peptide SN is involved in stimulating the production and release of LH (Zhao et al., 2011). Thus, granin family proteins and their derived peptides play important roles in hormone secretion. Accordingly, we propose that manserin regulates the body metabolic rate by modulating thyroid hormone secretion, although further experiments are necessary to resolve this issue.

The presence of manserin in only approximately one-third of parafollicular cells indicates that manserin may be a marker for one subtype of the parafollicular cells. Sawicki (1995) reported that somatostatin was present in only a subset of these cells. The characterization of functionally different subtypes of the parafollicular cells awaits further studies of thyroid manserin.

The manserin precursor, SgII, was present in almost all parafollicular cells, whereas manserin was found in only one subset. Most parafollicular cells contain prohormone convertase (PC) 1 and PC2, which cleave precursor proteins including SgII at paired basic sites to yield bioactive peptides that include SN, EM66, and manserin (Kurabuchi and Tanaka, 2002). The same authors reported that PC2 was equally distributed in all of the parafollicular cells, but that the content of PC1 was different among the parafollicular cells. One possibility is that manserin is produced by the cleavage of SgII by PC1 and is accordingly found only in the parafollicular cells expressing relatively higher levels of PC1.

Manserin localizes in TSH-expressing cells and follicular epithelial cells in the pituitary and thyroid glands, respectively. TSH activates follicular epithelial cells and stimulates synthesis and secretion of thyroid hormones, T3 and T4 (Szkudlinski et al., 2002). The production and secretion of TSH are suppressed by blood levels of thyroid hormones. Thus, blood TSH levels are tightly controlled by a negative-feedback loop. The presence of manserin in TSH-expressing cells and follicular epithelial cells suggests that it plays a role in the maintenance of homeostasis using this negative-feedback mechanism. Further investigations of manserin are required to resolve this question. Since manserin was shown to be expressed depending on the stress (Kamada et al., 2010), homeostasis of calcium regulation depending on the stress is also thought to be maintained through manserin. Further studies using stress animals should be necessary to resolve this issue.

As a result of this study, we conclude that the novel peptide manserin is localized in TSH-expressing cells in the adult rat pituitary gland and in follicular epithelial cells in the thyroid gland. Although the manserin precursor protein SgII was found in almost all parafollicular cells, manserin was found in only approximately one-third of these cells. These results suggest that manserin performs subtype-specific functions in the parafollicular cells.

References

Cheng SY, Leonard JL, Davis PJ. Molecular aspects of thyroid hormone actions. Endocr Rev 2010;31:139–70.

Foster GV. Calcitonin (thyrocalcitonin). N Engl J Med 1968;279:349–60.

Iacangelo AL, Eiden LE. Chromogranin A: current status as a precursor for bioactive peptides and a granulogenic/sorting factor in the regulated secretory pathway. Regul Pept 1995;58:65–88.

Ida-Eto M, Oyabu A, Ohkawara T, Tashiro Y, Narita N, Narita M. Existence of manserin, a secretogranin II-derived neuropeptide, in the rat inner ear; relevance to modulation of auditory and vestibular system. J Histochem Cytochem 2012;60:69–75.

Kamada N, Tano K, Oyabu A, Imura Y, Narita N, Tashiro Y, et al. Immunohistochemical localization of manserin, a novel neuropeptide derived from secretogranin II, in rat adrenal gland, and its upregulation by physical stress. Int J Pept Res Ther 2010;16:55–61.

Kim T, Tao-Cheng JH, Eiden LE, Loh YP. Chromogranin A, an "on/off" switch controlling dense-core secretory granule biogenesis. Cell 2001;106:499–509.

Kurabuchi S, Tanaka S. Immunocytochemical localization of prohormone convertases PC1 and PC2 in the mouse thyroid gland and respiratory tract. J Histochem Cytochem 2002;50:903–9.

Ohkawara T, Oyabu A, Ida-Eto M, Tashiro Y, Tano K, Nasu F, et al. Secretogranin II and its derivative peptide, manserin, are differentially localized in Purkinje cells and unipolar brush cells in the rat cerebellum. Int J Pept Res Ther 2011;17:193–9.

Ohkawara T, Shintani T, Saegusa C, Yuasa-Kawada J, Takahashi M, Noda M. A novel basic helix–loop–helix (bHLH) transcriptional repressor, NeuroAB, expressed in bipolar and amacrine cells in the chick retina. Brain Res Mol Brain Res 2004;128:58–74.

Sawicki B. Evaluation of the role of mammalian thyroid parafollicular cells. Acta Histochem 1995;97:389–99.

Sawicki B, Zabel M. Immunocytochemical study of parafollicular cells of the thyroid and ultimobranchial remnants of the European bison. Acta Histochem 1997;99:223–30.

Schmid KW, Kirchmair R, Ladurner D, Fischer-Colbrie R, Böcker W. Immunohistochemical comparison of chromogranins A and B and secretogranin II with calcitonin and calcitonin gene-related peptide expression in normal, hyperplastic and neoplastic C-cells of the human thyroid. Histopathology 1992;21:225–32.

Spitzweg C, Heufelder AE, Morris JC. Thyroid iodine transport. Thyroid 2000;10:321–30.

Szkudlinski MW, Fremont V, Ronin C, Weintraub BD. Thyroid-stimulating hormone and thyroid-stimulating hormone receptor structure–function relationships. Physiol Rev 2002;82:473–502.

Tano K, Oyabu A, Tashiro Y, Kamada N, Narita N, Nasu F, et al. Manserin, a secretogranin II-derived peptide, distributes in the rat endocrine pancreas colocalized with islet-cell specific manner. Histochem Cell Biol 2010;134:53–7.

Weiler R, Cidon S, Gershon MD, Tamir H, Hogue-Angeletti R, Winkler H. Adrenal chromaffin granules and secretory granules from thyroid parafollicular cells have several common antigens. FEBS Lett 1989;257:457–9.

Yajima A, Ikeda M, Miyazaki K, Maeshima T, Narita N, Narita M. Manserin, a novel peptide from secretogranin II in the neuroendocrine system. Neuroreport 2004;15:1755–9.

Yajima A, Narita N, Narita M. Recently identified a novel neuropeptide manserin colocalize with the TUNEL-positive cells in the top villi of the rat duodenum. J Pept Sci 2008;14:773–6.

Yoo SH, Chu SY, Kim KD, Huh YH. Presence of secretogranin II and high-capacity, low-affinity Ca^{2+} storage role in nucleoplasmic Ca^{2+} store vesicles. Biochemistry 2007;46:14663–71.

Zhao E, McNeilly JR, McNeilly AS, Fischer-Colbrie R, Basak A, Seong JY, et al. Secretoneurin stimulates the production and release of luteinizing hormone in mouse LβT2 gonadotropin cells. Am J Physiol Endocrinol Metab 2011;301:E288–97.

Journal of Neuroscience Research 00:00–00 (2014)

Action of Thyroxine on the Survival and Neurite Maintenance of Cerebellar Granule Neurons in Culture

Koshi Oyanagi,[1] Takayuki Negishi,[2] and Tomoko Tashiro[1]*

[1]Department of Chemistry and Biological Science, School of Science and Engineering, Aoyama Gakuin University, Kanagawa, Japan
[2]Department of Physiology, Faculty of Pharmacy, Meijo University, Nagoya, Japan

Developmental hypothyroidism causes severe impairments in the cerebellum. To understand the role of thyroid hormones (THs) in cerebellar development, we examined the effect of three different THs, thyroxine (T4), 3,5,3′-triidothyronine (T3), and 3,3′,5′-triiodothyronine (reverse T3; rT3), on the survival and morphology of cerebellar granule neurons (CGNs) in culture and found novel actions specific to T4. Rat CGNs obtained at postnatal day 6 were first cultured for 2 days in serum-containing medium with 25 mM K^+ (K25), then switched to serum-free medium with physiological 5 mM K^+ (K5) or with K25 and cultured for an additional 2 or 4 days. CGNs underwent apoptosis in K5 but survived in K25. Addition of T4 at concentrations of 100–200 nM but not T3 or rT3 rescued CGNs from cell death in K5 in a dose-dependent manner. Furthermore, 200 nM T4 was also effective in maintaining the neurites of CGNs in K5. In K5, T4 suppressed tau phosphorylation at two developmentally regulated sites as well as phosphorylation of c-jun N-terminal kinase (JNK) necessary for its activation and localization to axons. These results suggest that, during cerebellar development, T4 exerts its activity in cell survival and neurite maintenance in a manner distinct from the other two thyroid hormones through regulating the activity and localization of JNK.

Key words: cerebellar granule cells; thyroid hormones; cell survival; tau proteins; phosphorylation

Thyroid hormone (TH) is essential for the proper development of many organs, including the brain. Lack of sufficient TH during the perinatal period results in a syndrome termed *cretinism* in humans, which consists of severe impairment of body growth accompanied by mental retardation, ataxia, and deafness (Porterfield and Hendrich, 1993; Bernal, 2002). In the rodent models of perinatal hypothyroidism with growth retardation and neurological symptoms similar to human cretinism, characteristic morphological impairments in cell migration, dendritic arborization, and myelination are observed in the brain (Bernal and Nunez, 1995; Oppenheimer and Schwartz, 1997; Koibuchi and Chin, 2000; Thompson and Potter, 2000; Williams, 2008), leading to behavioral alterations (Negishi et al., 2005).

Structural and functional alterations resulting from perinatal hypothyroidism are most evident in the cerebellum, where major development takes place during the critical time window of TH action corresponding to the first 2 weeks after birth in rodents (Koibuchi et al., 2003; Anderson, 2008; Koibuchi, 2008). In hypothyroid animals, migration of cerebellar granule neurons (CGNs) from the external granular layer (EGL) to the internal granular layer (IGL) is severely retarded so that a thick EGL remains even at 2 weeks postnatally when the EGL has practically disappeared in euthyroid animals. Together with impaired development of Purkinje cell dendrites, synaptic connections between these dendrites and parallel fiber axons of CGNs are severely reduced in hypothyroidism. Although a limited number of genes involved in the thyroid hormone-dependent cerebellar development have been identified by global gene expression analyses (Quignodon et al., 2007; Takahashi et al., 2008; Chatonnet et al., 2012), this is still not adequate to explain the precise mechanisms underlying large physiological actions of TH. In addition, nongenomic action of TH utilizing cell surface receptors or cytoplasmic receptors has also been found in cerebellar astrocytes, Purkinje cells, and CGNs (Siegrist-Kaiser et al., 1990; Farwell et al., 1995, 2005; Kimura-Kuroda et al., 2002).

The present study investigates the effect of TH directly on rat CGNs in culture to understand how TH regulates the development of these cells. Unlike other types of neurons, CGNs obtained from the early postnatal

Additional Supporting Information may be found in the online version of this article.

Contract grant sponsor: Ministry of Health, Labor, and Welfare of Japan (to T.T.); Contract grant sponsor: MEXT-Supported Program for the Strategic Research Foundation at Private Universities, 2013–2017

*Correspondence to: Tomoko Tashiro, Department of Chemistry and Biological Science, School of Science and Engineering, Aoyama Gakuin University, 5-10-1 Fuchinobe, Chuo-ku, Sagamihara, Kanagawa 252-5258, Japan. E-mail: ttashiro@aoyamagakuin.jp

Received 9 June 2014; Revised 27 September 2014; Accepted 17 October 2014

Published online 00 Month 2014 in Wiley Online Library (wileyonlinelibrary.com). DOI: 10.1002/jnr.23519

rat cerebellum undergo apoptosis when cultured in serum-containing medium with a physiological concentration of K^+ (5 mM; low K^+), whereas they survive more than 2 weeks in serum-containing or serum-free medium with 25 mM K^+ (high K^+; Gallo et al., 1987; Yamagishi et al., 2001; Zhong et al., 2004). Such low-K^+-induced death of CGNs and its rescue by high K^+ has been studied extensively as a model of activity-dependent neuronal survival *in vivo*. Other than high-K^+-induced depolarization, growth factors such as insulin-like growth factor 1 and brain-derived neurotrophic factor have also been shown to protect CGNs from low-K^+-induced death (Yamagishi et al., 2003a; Bazan-Peregrino et al., 2007; D'Mello et al., 1997) through activation of the phosphoinositide 3-kinase/protein kinase B (Akt) pathway (Zhang et al., 1998; Yamagishi et al., 2003b; Zhong et al., 2004). Because TH is one of the candidate serum factors influencing survival of CGNs, this study examines the effect of three different forms of TH, thyroxine (T4), 3,5,3′-triidothyronine (T3), and 3,3′,5′-triiodothyronine (reverse T3; rT3), on the survival as well as the morphology of CGNs in culture. Our results show that T4 but not T3 or rT3 was effective in promoting survival of CGNs in serum-free, low-K^+ medium. T4 was also effective in maintaining CGN neurites in K5 by stabilizing microtubules through reduction of tau phosphorylation at least at two developmentally regulated phosphorylation sites.

MATERIALS AND METHODS

Animals

Pregnant Wistar ST rats were purchased from SLC (Shizuoka, Japan) and were maintained under controlled conditions (24°C ± 1°C) on a 12-hr light (0600–1800 hr)/12-hr dark (1800–0600 hr) cycle. Food and water were freely available. All animal treatments were approved by the Animal Experimentation Committee of Aoyama Gakuin University and were carried out under veterinary supervision in accordance with the Society for Neuroscience Guidelines for the use of animals in neuroscience research.

Primary Culture of CGNs

Cerebelli from postnatal day (P) 6 rats were transferred to ice-cold isolation medium consisting of equal volumes of Ca^{2+}- and Mg^{2+}-free phosphate-buffered saline (PBS) and Dulbecco's modified Eagle's medium (DMEM)/F-12 (1:1; Gibco, Palo Alto, CA), cut into small pieces, freed of meninges, and digested with 0.25% trypsin (Gibco) in PBS at 37°C for 30 min. Cells were dissociated gently by passages through a disposable pipette and centrifuged twice in a serum-containing medium (DMEM/F-12 supplemented with 10% fetal bovine serum [FBS]) at 800 rpm for 5 min at room temperature (r.t.). The cells were resuspended in serum-containing medium with 25 mM KCl, 1.0% insulin–transferrin–selenium (ITS-X; Gibco), 10 U/ml penicillin, and 10 μg/ml streptomycin (Gibco) and plated onto a 96-well plate, a four-well plate, a 3.5-cm dish, or a 16-well slide chamber coated with poly-L-lysine (Gibco) at 3,000 cells/mm^2. All cultures were maintained at 37°C in 95% humidified air and 5% CO_2. At 24 hr after plating, 5 μM cytosine arabinoside was added and left in the medium throughout the culture period to eliminate proliferative cells. To examine the effect of thyroid hormones, the cells were further cultured for up to 4 days in serum-free high-K^+ medium (K25; DMEM/F-12 containing 25 mM KCl, 1.0% ITS-X, penicillin, and streptomycin) or low-K^+ medium (K5; DMEM/F-12 containing 5 mM KCl, 1.0% ITS-X, penicillin, and streptomycin) with or without thyroid hormones L-thyroxine (T4), 3,5,3′-L-triiodothyronine (T3), or 3,3′,5′-triiodothyronine (reverse T3; rT3; Sigma-Aldrich, St. Louis, MO).

Cerebellar Slice Cultures

After decapitation, brains of P7 rats were dissected out into isolation medium. Sagittal slices (300-μm thickness) of the cerebellum were cut with a Microslicer (Dosaka EM, Kyoto, Japan) and then placed on Millicell-CM culture inserts (Merck-Millipore, Billerica, MA) in medium containing 20% FBS and penicillin–streptomycin. After 2 days of culture in serum-containing medium, the slices were transferred to K25 or K5.

Assessment of Cell Viability

The viability of cells cultured for 48 hr in 96-well plates under various conditions was assessed by measuring mitochondrial metabolic activity with a CellTiter-Blue cell viability assay kit (Promega, Fitchburg, WI). CellTiter-Blue reagent was added directly to cells cultured in 96-well plates and incubated for 30 min at 37°C. After incubation, fluorescence (560_{Ex}/590_{Em}) was recorded with a Fluoroskan Ascent FL (Thermo Labsystems, Beverly, MA). Results are expressed as percentages of the value obtained from cells cultured in the control K25 medium without TH.

Hoechst 33258 dye (Sigma-Aldrich) was used to identify dead cells with pyknotic nuclei. After fixation with a 4% paraformaldehyde (PFA)−8% sucrose solution in PBS, cultured cells in 16-well chamber slides were permeabilized with 0.2% Triton X-100 (Sigma-Aldrich) solution and incubated with 0.2 μg/ml Hoechst 33258 for 1 hr at r.t. to detect pyknotic nuclei. Cells were examined under a fluorescence microscope (Axioplan 2; Carl Zeiss, Oberkochen, Germany). Microscopic images were obtained with a color CCD camera (ProgRes CFscan; Jenoptic, Jena, Germany), and the number of pyknotic nuclei was counted.

Apoptotic cells in cultured slices were detected by TUNEL assay with a DeadEnd fluorometric TUNEL system (Promega). Briefly, slices that had been cultured for 48 hr in K25 or K5 were transferred to microtubes and fixed for 1 hr at 4°C in PBS containing 4% PFA and 8% sucrose. The slices were then permeabilized with 0.2% Triton X-100 in PBS and incubated for 1 hr at 37°C in rTdT enzyme and Nucleotide Mix solution. After termination of the enzyme reaction, slices were transferred onto glass slides, sealed with Dako fluorescent mounting medium (Dako, Carpinteria, CA), and examined under an Axioplan 2 fluorescence microscope. Microscopic images were captured with a ProgRes CFscan color CCD camera.

Western Blotting

Cell homogenate was obtained by scraping the cells off and sonicating for 10 sec in sodium dodecyl sulfate (SDS)

sample buffer (50 mM Tris, 2.0% SDS, 10% glycerol, 10% 2-mercaptoethanol, and bromophenol blue) containing protease and phosphatase inhibitors (Roche Applied Science, Indianapolis, IN). After having been boiled for 3 min, proteins in the homogenates were resolved by SDS-polyacrylamide gel electrophoresis (PAGE) and transferred to polyvinylidene fluoride membrane (Immobilon P; Millipore). The blots were blocked with 2.5% nonfat dry milk or 2% BSA in Tris-buffered saline containing 0.1% Tween20 (TBS-T) and incubated at 4°C overnight with one of the following primary antibodies: anti-microtubule-associated protein (MAP) 2 (mouse monoclonal; 1:2,000), anti-β-actin (mouse monoclonal; 1:50,000; Sigma-Aldrich), anti-$GABA_A$ receptor α-1 (rabbit polyclonal; 1:1;000; Thermo Scientific, Waltham, MA); anti-human contactin-2/TAG1 (goat polyclonal; 1:2,000; R&D Systems, Minneapolis, MN); anti-tau, clone Tau-5 (mouse monoclonal; 1:5,000), anti-β-tubulin (mouse monoclonal; 1:1,000) from Merck-Millipore; anti-Tau pS199 phosphospecific antibody (rabbit polyclonal; 1:2,000; Invitrogen, Carlsbad, CA); anti-phospho-MAPT (pSer422; rabbit polyclonal; 1:1,000; Sigma-Aldrich); anti-glycogen synthase kinase 3β (GSK-3β; mouse monoclonal; 1:10,000; BD Transduction Laboratories, San Jose, CA); anti-phospho-GSK-3β (Ser9; 5B3; rabbit monoclonal; 1:10,000), anti-stress-activated protein kinase (SAPK)/c-jun N-terminal kinase (JNK; 56G8; rabbit monoclonal; 1:1,000), anti-phospho-SAPK/JNK (Thr183/Tyr185; 81E11; rabbit monoclonal; 1:1,000), anti-phospho-Akt (Ser473; 193H12; rabbit monoclonal; 1:5,000), anti-phospho-Akt (Thr308; C31E5E; rabbit monoclonal; 1:2,000) from Cell Signaling Technology (Danvers, MA), or anti-Akt1/2/3 (H-136; rabbit polyclonal; 1:500; Santa Cruz Biotechnology, Santa Cruz, CA). After they were rinsed in TBS-T, the blots were further incubated with horseradish peroxidase (HRP)-conjugated secondary antibodies (1:5,000; Jackson Immunoresearch, West Grove, PA) and visualized by exposure to Hyperfilm ECL (GE Healthcare, Piscataway, NJ) with Immobilon Western Chemiluminescent HRP substrate (Millipore). For quantification, the films were scanned, the density of each band was measured in Image J (NIH), and the results were normalized with β-actin as standard.

Immunocytochemistry

Cells in 16-well chamber slides were fixed with PBS containing 4% paraformaldehyde (PFA) and 8% sucrose for 5 min at 4°C, rinsed in PBS, and postfixed for 2 min in methanol at −20°C. Fixed cells were blocked in blocking buffer (4% normal goat serum, 2% BSA, and 0.2% Triton X-100 in PBS) for 30 min at r.t. and incubated with antitau antibody, clone Tau-5 (1:500; Millipore), anti-MAP2 antibody (1:500; Sigma-Aldrich), anti-SAPK/JNK (56G8; rabbit monoclonal; 1:1,000), and anti-phospho-SAPK/JNK (Thr183/Tyr185; 81E11; rabbit monoclonal; 1:1,000) overnight at 4°C. They were further incubated with Alexa 488-conjugated anti-mouse IgG (1:500; Invitrogen), Alexa 546-conjugated anti-rabbit IgG (1:500; Invitrogen), or Alexa 488-conjugated anti-rabbit IgG (1:500; Invitrogen), and Hoechst 33258 (0.1 μg/ml; Sigma-Aldrich) for 1 hr at r.t. The slides were observed under a Axioplan 2 fluorescence microscope, and the images were recorded with a ProgRes color CCD camera.

Analysis of Actin and Tubulin Polymerization

Cells cultured in ϕ3.5-cm dishes in serum-containing high-K^+ medium for 2 days were transferred to K25, K25 with 200 nM T4, or K5 with 200 nM T4 and incubated for an additional 48 hr. After incubation, cells were rinsed with ice-cold PBS and homogenized in separation buffer (5 mM Tris, pH 8.0, 1 mM EDTA, 0.5% Triton X-100 with protease inhibitor cocktail [Sigma-Aldrich]). The homogenate was centrifugated at 100,000*g* for 1 hr at 4°C to yield supernatant and precipitate fractions. Ice-cold trichloroacetic acid was added to both supernatant and precipitate fractions homogenized in separation buffer to give final concentrations of 10%. After incubation for 30 min on ice, proteins in both fractions were recovered as precipitates by centrifugation at 12,000*g* for 5 min at 4°C. Precipitated proteins were rinsed with ice-cold ethanol three times, dissolved in SDS sample buffer by homogenization, and boiled for 5 min. The amount of β-actin and β-tubulin recovered in each supernatant or precipitate fraction was further analyzed by SDS-PAGE and Western blotting as described above.

Statistical Analysis

Values are given as mean ± SEM. Differences between the two experimental groups were evaluated by Student's *t*-test. In the case of three or more groups, Tukey's test was used. For analysis of cell viability, two-way ANOVA followed by Dunnett's multiple-comparisons test was used. In all cases, $P < 0.05$ was considered statistically significant.

RESULTS

Susceptibility of Differentiated CGNs to Low-K^+-Induced Cell Death

Sensitivities of CGNs to low-K^+-induced cell death were first compared among cells obtained from P1 rats (P1 cells) and P6 rats (P6 cells). P1 and P6 cells were initially cultured for 48 hr in high-K^+ medium containing 25 mM KCl and supplemented with 10% FBS, then transferred to serum-free high-K^+ medium containing 25 mM KCl (K25) or serum-free low-K^+ medium containing 5 mM KCl (K5). When cells were evaluated 48 hr later by mitochondrial reducing capacity, a significant reduction was observed in viability of cells cultured in K5 compared with those cultured in K25 with P6 cells, whereas P1 cells were equally viable in either medium (Fig. 1A). Viability of P6 cells in K5 decreased to 50% of those cultured in K25 within the first 2 days after switching to serum-free K5, reaching a plateau level at 4 days (Fig. 1B).

To examine the effect of K^+ concentration on the survival of CGNs in a more intact system, sagittal slices were prepared from the rat cerebellum at P7. At this age, thick EGL and IGL were clearly distinguishable such that responses of both proliferative cells in the EGL and post-migratory cells in the IGL could be studied in the same slice (Fig. 1C). After 2 days of culture in serum-containing K25, slices were transferred to serum-free K5

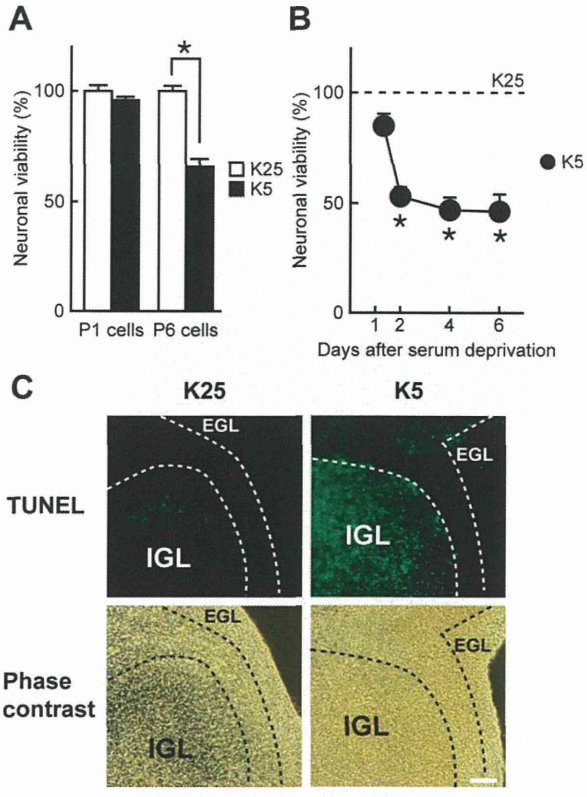

Fig. 1. Susceptibility of CGNs at different developmental stages to low-K^+-induced death. **A:** Low-K^+-induced death of CGNs prepared from rats at P1 (P1 cells) or P6 (P6 cells). K25, serum-free high-K^+ medium (open columns); K5, serum-free low-K^+ medium (solid columns). Values are mean ± SEM (n = 8). $\star P < 0.05$ between K5 and K25. **B:** Time dependence of low-K^+-induced cell death in CGNs prepared from rats at P6. Neuronal viability was assessed by mitochondrial reducing capacity. Values are mean ± SEM (n = 8). $\star P < 0.05$ between K5 and K25. **C:** Apoptotic cell death detected by TUNEL staining in P7 rat cerebellar slices cultured in K25 or K5 for 48 hr. Scale bar = 100 μm.

or K25 and cultured for an additional 2 days, and the extent of cell death was analyzed by TUNEL staining. As shown in Figure 1C, a large amount of TUNEL-positive cells was observed in slices cultured in K5 but not in K25. TUNEL-positive cells in K5 slices were observed exclusively in the IGL. These results indicate that only postmigratory CGNs located in the IGL are susceptible to low-K^+-induced cell death.

T4 but not T3 or rT3 Prevents the Death of CGNs Induced by Low K^+

To test whether thyroid hormone has an effect on this low-K^+-induced death of CGNs in primary culture, P6 cells were cultured as described above in high-K^+ medium containing 10% FBS for 2 days, then switched to either K5 or K25 containing one of the three different forms of TH, T4, T3 or rT3, at varying concentrations (Fig. 2A–C). When cells were evaluated 48 hr after switching to K5, a dose-dependent increase in cell viability was observed with T4 concentrations of 100–200 nM (Fig. 2A) but not with similar or higher concentrations of T3 (Fig. 2B) or rT3 (Fig. 2C). With 200 nM T4 in K5, cells were fully protected from low-K^+-induced death. In K25, cell viability was not affected by the addition of any TH.

The effect of T4 was further confirmed by visualizing chromatin condensation of dyeing cells with Hoechst 33258 staining (Fig. 2D). Large numbers of cells with brightly stained pyknotic nuclei were observed when CGNs were cultured in K5, which was markedly reduced by the addition of T4 (200 nM) but not T3 (200 nM; Fig. 2D). In the presence of T4 in K5, the number of cells with pyknotic nuclei was comparable to that observed in K25 (Fig. 2E).

Because only postmigratory CGNs were susceptible to low-K^+-induced cell death, we next examined whether the developmental stage of CGNs was altered by the addition of T4 by using $GABA_A$ receptor α1 subunit (GABRα1), which is developmentally upregulated *in vivo*, and transient axonal glycoprotein-1 (TAG-1), which is expressed only in the postmitotic, premigratory cells in the EGL as indicators (Fig. 2F–H). As shown in Figure 2F,G, expression of GABRα1 increased with days in culture in K25 without T4. Addition of T4 to K25 (K25 + T4) or K5 (K5 + T4) resulted in significantly larger increases in GABRα1 immunoreactivity after 2 days than K25 alone. After 4 days in culture, GABRα1 expression levels were comparable among the three culture conditions. Expression of TAG-1, on the other hand, time dependently decreased under these three culture conditions (Fig. 2F,H).

The results show that maturation of CGNs proceeded normally in the presence of T4 with a slight enhancement of GABRα1 expression. It is thus clear that T4 did not protect CGNs from low-K^+-induced cell death by interfering with their maturation.

Effect of T4 on the Neurites of CGNs

We next examined the effect of 200 nM T4 on the neurites of CGNs by immunofluorescent staining with antibodies against the two major MAPs of neurites, MAP2 and tau. As shown in Figure 3, more neurites were visualized with anti-tau staining than with anti-MAP2 staining, indicating the axonal nature of the neurites (Takemura et al., 1991). Addition of T4 to K5 not only promoted cell survival but was also effective in maintaining a network of neurites comparable to that observed in K25. Addition of T4 to K25, on the other hand, resulted in an apparently denser network of tau-positive neurites compared with cells in K25 alone or K5 + T4, which was further confirmed by Western blotting (see Fig. 5D below).

Effect of T4 on the Polymerization of Actin and Tubulin

The following experiments compared the CGNs cultured under the three different conditions that fully sustained cell survival for 48 hr, K25, K25 + T4, and K5 + T4. First, the expression as well as the

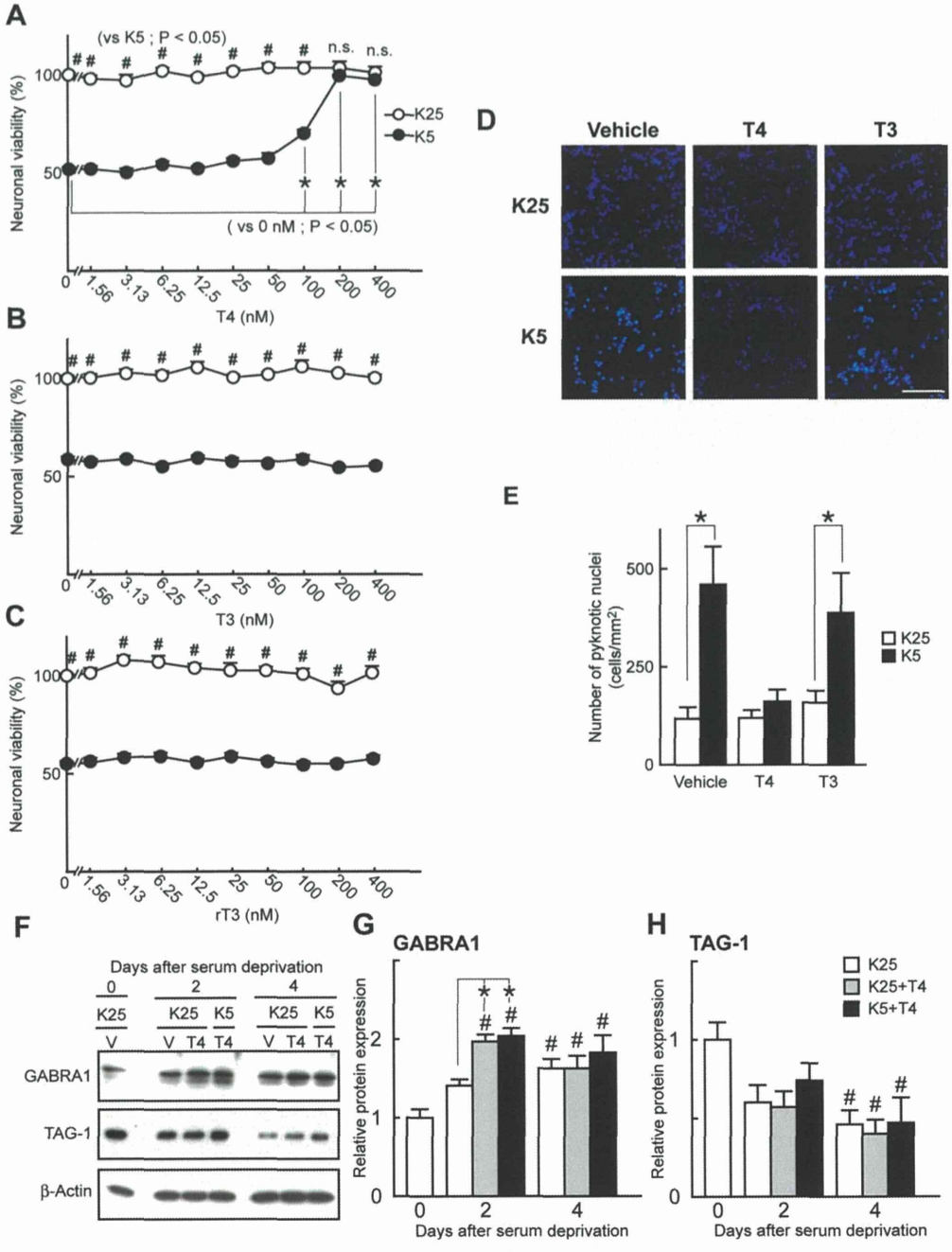

Fig. 2. Effect of thyroid hormones on low-K^+-induced death of CGNs. **A–C:** Neuronal viability of P6 cells cultured for 48 hr in K25 (open circles) or K5 (solid circles) containing various concentrations of T4 (A), T3 (B), or rT3 (C). Values are expressed relative to that of cells cultured in K25 without each hormone. Values are mean ± SEM (n = 12). $^{\star}P < 0.05$ vs. K5 without each hormone; $^{\#}P < 0.05$ between K25 and K5 containing the same dose of each hormone; n.s. in 200 and 400 nM T4 indicates no significant effect of low-K^+ stimulation, i.e., full protection by T4 from low-K^+-induced cell death. **D:** Fluorescent images of pyknotic nuclei visualized by Hoechst 33258 in CGNs cultured in K25 (upper row) or K5 (lower row) with or without 200 nM T4 (middle column) or T3 (right column). **E:** Number of cells with pyknotic nuclei per unit area (mm^2) in CGNs cultured in K25 (open columns) or K5 (solid columns) with or without 200 nM T4 or T3. Values are mean ± SEM (n = 16–20). $^{\star}P < 0.05$ between two values indicated. **F:** Representative immunoblots of GABRα1 and TAG-1 in CGNs cultured for 0, 2, or 4 days in K25 or K5 in the presence or absence of 200 nM T4. Day 0 indicates a sample just before switching to serum-free medium. **G,H:** Protein expression of GABRα1 (G) and TAG-1 (H) in CGNs cultured for 0, 2, or 4 days in K25 (open columns), K25 containing 200 nM T4 (K25 + T4; gray columns), or K5 containing 200 nM T4 (K5 + T4; solid columns). β-Actin was used as loading control. Values are expressed as relative to day 0 and are mean ± SEM (n = 4). $^{\star}P < 0.05$ vs. K25 alone on the same day; $^{\#}P < 0.05$ vs. day 0. Scale bar = 100 μm. [Color figure can be viewed in the online issue, which is available at wileyonlinelibrary.com.]

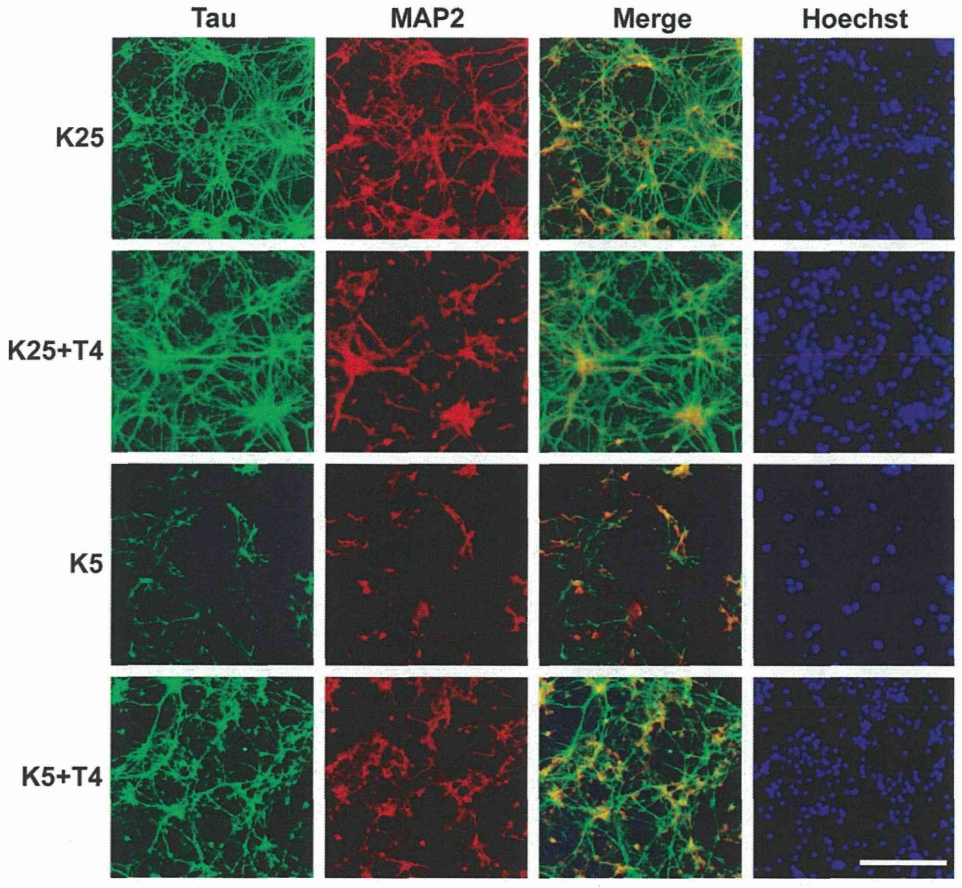

Fig. 3. Effect of T4 on neurites of cultured CGNs. Immunofluorescent images of CGNs cultured for 48 hr in K25 or K5 with or without 200 nM T4 with anti-tau (green) and anti-MAP2 (red) antibodies. Hoechst 33258 was used to stain nuclei. Scale bar = 50 μm.

polymerization state of major cytoskeletal proteins, β-tubulin and β-actin, were evaluated by separating 0.5% Triton X-100 homogenate of harvested cells into supernatant and precipitate fractions containing unpolymerized and polymerized cytoskeletal proteins, respectively. Total amounts of β-tubulin or β-actin were comparable among CGNs cultured in K25, K25 + T4, and K5 + T4 (Fig. 4A,B). The proportion of polymerized tubulin was increased more than twofold by the addition of T4 in K25 (Fig. 4C), whereas the proportion of polymerized actin did not differ significantly (Fig. 4D). Tubulin polymerization seemed to increase slightly in CGNs cultured in K5 + T4.

Effect of T4 on the Expression and Phosphorylation of MAPs

MAP2 consists of high-molecular-weight isoforms, MAP2a and MAP2b, and a lower molecular weight, juvenile isoform, MAP2c, which are produced from a single gene by alternative splicing. Expression levels of these three MAP2 isoforms were comparable among CGNs cultured for 2 days in K25, K25 + T4, and K5 + T4 (Fig. 5A–C). After 4 days of culture, however, MAP2a and 2b tended to be increased in the presence of T4 both in K25 and in K5. At the same time, a significant reduction in MAP2c was observed in K25 + T4 compared with K25 alone (Fig. 5C), suggesting that T4 enhanced maturation of MAP2 isoform composition in cultured CGNs.

In the case of tau, although six splicing isoforms can be produced from a single gene, only the lowest molecular weight, juvenile isoform (54 kDa) was observed in CGNs cultured under all three conditions (Fig. 5A). The amount of tau increased approximately twofold in CGNs cultured for 2 days in the presence of 200 nM T4 both in K25 and in K5 (Fig. 5A,D). After 4 days of culture, however, a significant increase in tau expression remained only in cells cultured in K25 + T4.

Because the ability of tau to promote microtubule assembly and stabilization is regulated by its phosphorylation, the effect of T4 on the phosphorylation of tau was further analyzed. Among the many phosphorylation sites of tau protein, two developmentally regulated sites, Ser422 and Ser199, as well as two sites known to be hyperphosphorylated in PHF tau, Ser396 and Thr231, were examined (Yu et al., 2009).

Tau phosphorylated at Ser422 (p-Tau Ser422) showed significant changes in amount by the addition of

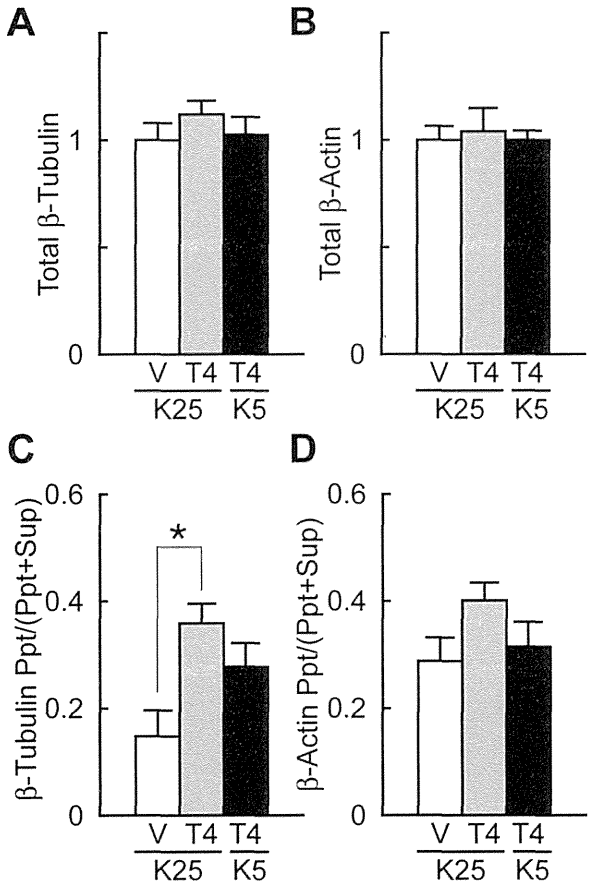

Fig. 4. Effect of T4 on the polymerization of β-tubulin and β-actin in cultured CGNs. **A,B:** Quantification of protein expression of total β-tubulin (A) and total β-actin (B) in extracts obtained from CGNs cultured for 48 hr in K25 (open columns), K25 containing 200 nM T4 (K25 + T4; gray columns), or K5 containing 200 nM T4 (K5 + T4; solid columns), in which each value is expressed relative to those of cells cultured in K25. **C,D:** Level of polymerization of β-tubulin (C) and β-actin (D) in CGNs. Sup and Ppt indicate unpolymerized supernatant and polymerized precipitate fractions of Triton X-100 extracts separated by ultracentrifugation (see Materials and Methods). Extent of polymerization was expressed as the proportion of the protein in Ppt against the sum of the protein in Ppt and Sup. Values are mean ± SEM (n = 4). $*P < 0.05$ vs. K25.

T4. After 2 days of culture, p-Tau Ser422 was increased 1.7-fold and 2.2-fold in K25 + T4 and K5 + T4, respectively, compared with that in K25 (Fig. 5E). Between days 2 and 4, however, p-Tau Ser422 increased more than 2.5-fold in CGNs cultured in K25, whereas it remained at the same level in K25 + T4 and decreased tenfold in K5 + T4. On the other hand, the phosphorylation level (p-Tau Ser422/total Tau) at this site was comparable under the three culture conditions after 2 days in culture but was significantly reduced after 4 days in both K25 and K5 containing T4 (Fig. 5F). In K5 + T4, a severe reduction in the amount of p-Tau Ser422 contributed to the reduction in phosphorylation level, whereas in K25 + T4 an increase in total tau (Fig. 5D) was responsible for the apparent reduction in the phosphorylation level instead of an actual decrease in the amount of p-Tau Ser422. In contrast, there was no apparent change in tau phosphorylated at Ser199 (p-Tau Ser199) by T4 addition in either K25 or K5 (Fig. 5G), but the phosphorylation level at this site was reduced by 50% after 2 days in culture in both K25 and K5 (Fig. 5H) because of twofold increases of total tau in the presence of T4 (Fig. 5D). A significant reduction in the phosphorylation level at Ser199 remained in K25 + T4 after 4 days in culture for the same reason.

Under all three culture conditions, tau phosphorylated at Ser396 probed with one of the anti-PHF tau antibodies, PHF13, and tau phosphorylated at Thr231 probed with anti-Alzheimer's disease tau antibody, AT180, were not detected (data not shown).

Effect of T4 on GSK-3β and JNK

It is well known that tau is phosphorylated by a number of kinases, including GSK-3β, JNK, and cyclin-dependent kinase-5. Among these, kinases reported to be responsible for the phosphorylation at Ser199 and Ser422 are GSK-3β and JNK, respectively. Therefore, we examined the effect of T4 on the activation of these two kinases.

Kinase activity of GSK-3β is downregulated by phosphorylation at Ser9. As shown in Figure 6A, phosphorylation at this site was observed in CGNs cultured for 2 or 4 days under all three conditions. CGNs cultured for 2 days in K25 + T4 transiently exhibited a higher level of phosphorylation compared with cells in K25 or K5 + T4 (Fig. 6A). A major kinase phosphorylating GSK-3β and suppressing its activity is Akt, which is known to be activated by phosphorylation at both Ser473 and Thr308. As shown in Figure 6B, Akt phosphorylation at each of these sites was transiently enhanced by the addition of T4 to K25 after 2 days but was back to the level of K25 alone after 4 days. A similar tendency was observed in K5 + T4. Transient enhancement of Akt phosphorylation in K25 + T4 thus matched in timing with the transient phosphorylation of GSK-3β observed under the same culture condition (Fig. 6A). Each of the three subtypes of JNK, JNK1–3, or MAPK8~10 consists of several splice variants with molecular weights of 46 kDa (P46) and 54 kDa (P54), all of which are activated by simultaneous phosphorylation at Thr183 and Tyr185 (for review see Kyriakis and Avruch, 2012). In differentiating neurons, a major pool of phosphorylated, active JNK (p-JNK) localizes to neurites, where it plays a critical role in axon determination and axon guidance through regulation of microtubule stability (Oliva et al., 2006; Hirai et al., 2011; Qu et al., 2013). Under all three culture conditions, an antibody against p-JNK stained the neurites, whereas an antibody against total JNK stained mainly the cell bodies, with much weaker staining of the neurites (Fig. 7A). Immunoblotting analysis revealed that the amount of total JNK was comparable among the three culture conditions, whereas p-JNK was significantly

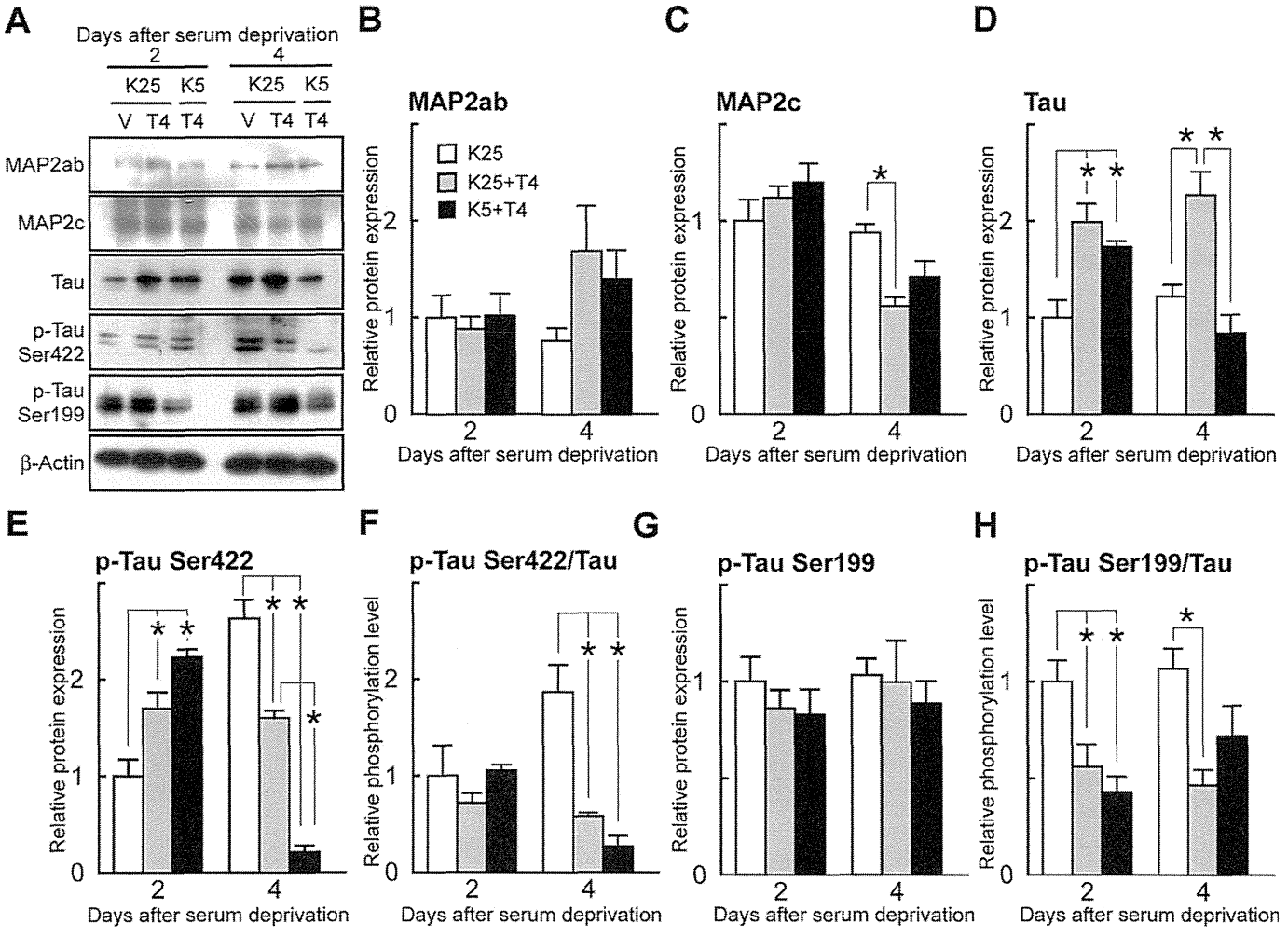

Fig. 5. Effect of T4 on the expression and phosphorylation of MAP2 and tau in cultured CGNs. **A:** Representative immunoblots of MAP2, tau, p-Tau Ser422, and p-Tau Ser199 in CGNs cultured for 2 or 4 days in K25, K25 containing 200 nM T4 (K25 + T4), or K5 containing 200 nM T4 (K5 + T4). β-Actin was used as loading control. **B–D:** Amount of MAP2a,b (B), MAP2c (C), or tau (D) in CGNs cultured for 2 or 4 days in K25 (open columns), K25 containing 200 nM T4 (K25 + T4; gray columns), or K5 containing 200 nM T4 (K5 + T4; solid columns) expressed relative to that of CGNs cultured for 2 days in K25. Values are mean ± SEM (n = 4). $*P < 0.05$ in pairwise comparisons. **E–H:** Amount of p-Tau Ser422 (E), phosphorylation level at Ser422 (F), amount of p-Tau Ser199 (G), and phosphorylation level at Ser199 (H) in CGNs cultured for 2 or 4 days in K25 (open columns), K25 containing 200 nM T4 (K25 + T4; gray columns), or K5 containing 200 nM T4 (K5 + T4; solid columns) expressed relative to that of CGNs cultured for 2 days in K25. Values are mean ± SEM (n = 4). $*P < 0.05$ in pairwise comparisons.

decreased in amount in K5 + T4 after 2 and 4 days of culture (Fig. 7B).

DISCUSSION

Effect of T4 on Cell Survival and Neurite Maintenance of CGNs Cultured in K5 and K25

The present study shows that T4 but not T3 or rT3 is effective in promoting survival of CGNs in serum-free, low-K^+ medium (K5). T4 not only served as a survival factor, but was also effective in fully maintaining the neurites of CGNs in K5 by stabilizing microtubules through reduction of tau phosphorylation at least at two developmentally regulated sites, Ser199 and Ser422. T4 in K5 downregulated the activities of the two tau kinases responsible for phosphorylation of these sites, GSK-3β and JNK, by maintaining inhibitory phosphorylation of GSK-3β as in the case of other growth factors and, in addition, by suppressing phosphorylation of JNK necessary for its activation. Given that these kinases are involved in low-K^+-induced death of CGNs (Yamagishi et al., 2001, 2003b; Zhong et al., 2004; Song et al., 2010), suppression of their activities is likely to be a key to the function of T4 in both cell survival and neurite maintenance in K5. JNK, in particular, is a good candidate for a T4 effector in the regulation of both processes because it has been shown to have a dual role in neurons as an SAPK and a kinase with developmental roles (Coffey et al., 2000, 2002). p-JNK is localized predominantly to neurites of developing neurons and plays critical roles

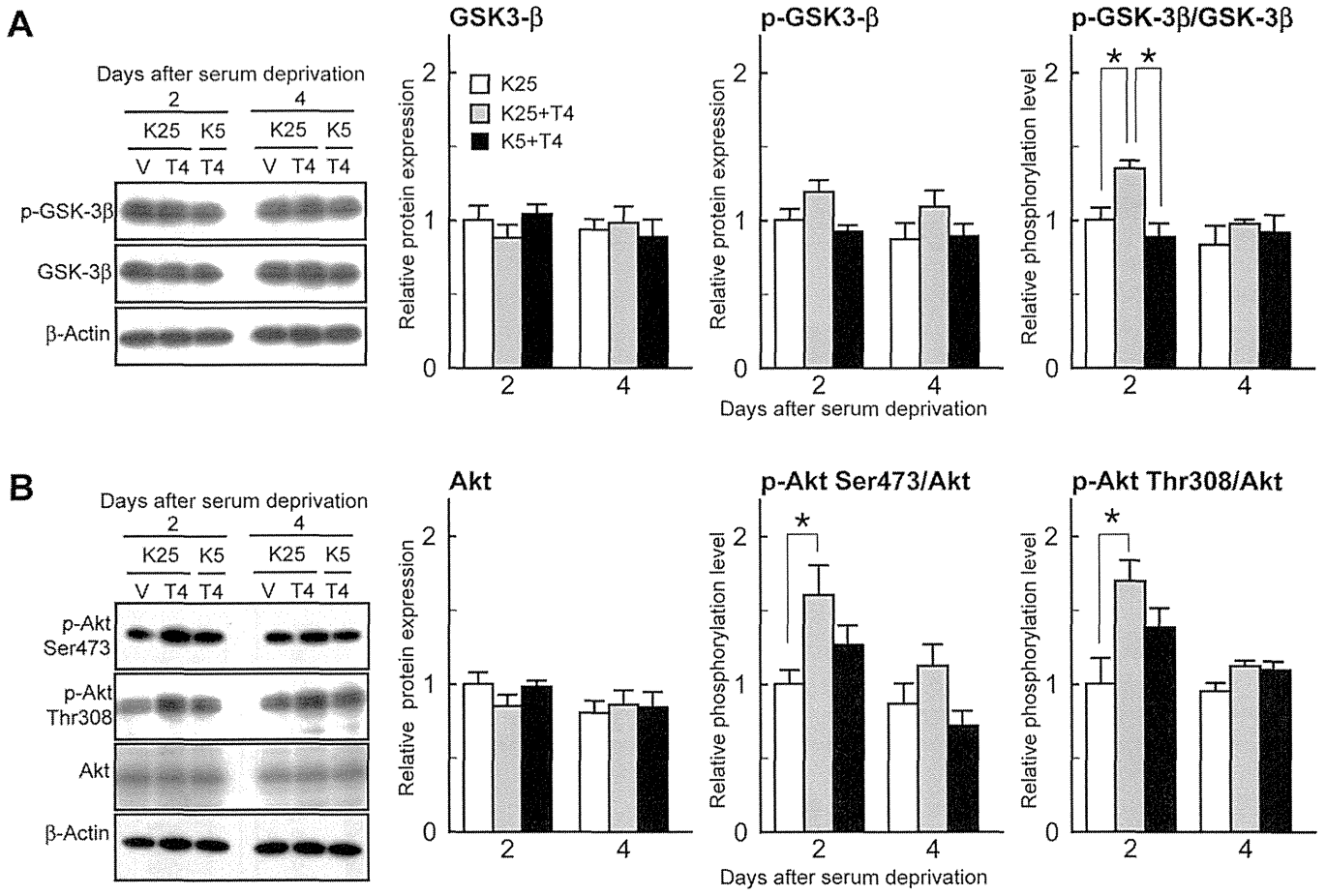

Fig. 6. Effect of T4 on the phosphorylation of GSK-3β and Akt in cultured CGNs. **A,B:** Representative immunoblots and quantification of the phosphorylation levels of GSK-3β at Ser9 (A) and Akt at Ser473 or Thr308 (B) in CGNs cultured for 2 or 4 days in K25 (open columns), K25 containing 200 nM T4 (K25 + T4; gray columns), or K5 containing 200 nM T4 (K5 + T4; solid columns) expressed relative to that of CGNs cultured for 2 days in K25. β-Actin was used as loading control. Values are mean ± SEM (n = 4). $*P < 0.05$ between the two values indicated.

in axon determination and axon guidance by regulating microtubule stability (Oliva et al., 2006; Hirai et al., 2011; Qu et al., 2013). Although phosphorylation of tau was not examined in these previous studies, tau is a likely candidate substrate of p-JNK in the regulation of microtubule stability because it is the major MAP in axons. Gene targeting studies have further demonstrated that JNK1 plays essential roles *in vivo* in neuronal migration and establishment of axon tracts (Chang et al., 2003; Hirai et al., 2006, 2011).

Addition of T4 to K25 induced an apparent reduction in the phosphorylation level of tau at both Ser199 and Ser422, but it was due mainly to an increase in total tau rather than a decrease in tau phosphorylation (Fig. 5). Given that an enhancement in Akt activation was observed in K25 + T4 after 2 days, activation of the mammalian target of rapamycin pathway might be involved in the upregulation of tau synthesis (Swiech et al., 2008; Tang et al., 2013; Westerholz et al., 2013) under this condition. Response of JNK toward T4 was also different in K5 and K25. In K5 + T4, p-JNK was significantly reduced after 4 days, whereas, in K25+T4, it tended to be increased (Fig. 6). Tau mRNA is particularly enriched in CGNs, with the peak of expression in the second and third postnatal weeks in the IGL (Takemura et al., 1991), at the time when CGN neurites are maturing into parallel fiber axons. T4-induced increase in total tau, together with the sustained activation of JNK in K25, might represent the actively elongating phase of CGN axons in the presence of T4 under depolarizing conditions.

Comparison of Survival-Promoting Activity With Typical Nongenomic Actions of T4

The survival-promoting activity of T4 described here is likely to be based on nongenomic action, given that the transcriptionally active T3 was without effect. Typically, nongenomic actions of TH have been defined as involving T4 and rT3 rather than T3, occurring within minutes to hours, and being mediated by cell surface

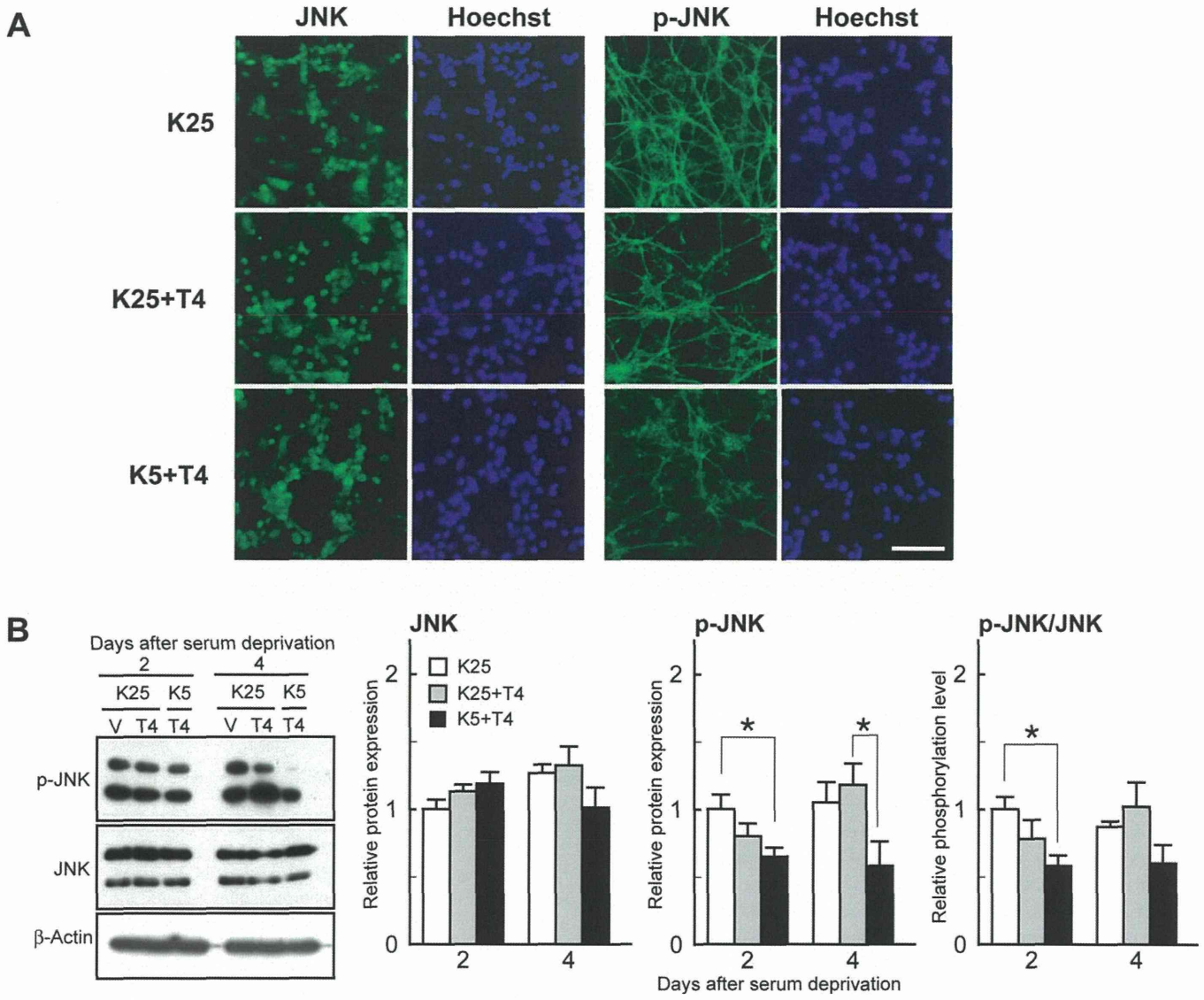

Fig. 7. Effect of T4 on the phosphorylation of JNK in cultured CGNs. **A:** Immunofluorescent images of CGNs cultured for 48 hr in K25, K25 with 200 nM T4 (K25 + T4), and K5 with 200 nM T4 (K5 + T4) with anti-JNK and anti-p-JNK antibodies. Hoechst 33258 was used to stain nuclei. **B:** Representative immunoblots and quantification of the phosphorylation levels of JNK in CGNs cultured for 2 or 4 days in K25 (open columns), K25 containing 200 nM T4 (K25 + T4; shaded columns), or K5 containing 200 nM T4 (K5 + T4; solid columns) expressed relative to that of CGNs cultured for 2 days in K25. β-Actin was used as loading control. Values are mean ± SEM (n = 4). $\star P < 0.05$ between the two values indicated. Scale bar = 50 μm.

receptors or nuclear receptors localized to the cytoplasm (for review see Farwell et al., 2006; Davis et al., 2008; Cheng et al., 2010). Because cell survival cannot be evaluated within such a short time span, we examined the rapid effect of T4, T3, and rT3 on the survival kinase Akt/PKB in CGNs cultured in K5 (Supp. Info. Fig. 1). The results show that T4 and T3 differentially affect the phosphorylation of Akt at Ser473 and Thr308, suggesting that distinct pathways are stimulated by each TH. Further studies are required, however, to determine how these initial responses are linked to cell survival or to cell death observed after 48 hr.

One of the well-known nongenomic actions of T4 is the rapid enhancement of actin polymerization first observed within 10 min after T4 addition in astrocytes cultured on a laminin-coated surface (Siegrist-Kaiser et al., 1990). Although to a lesser extent, T4 and rT3 were also shown to be effective in increasing F-actin content of CGNs examined 16 hr after TH addition and in inducing neurite outgrowth as well as migration of CGNs out of cerebellar explants (Farwell et al., 2005). Under the present experimental conditions, however, enhancement of actin polymerization was not observed with any TH at 0.5, 1, or 4 hr after addition (Supp. Info. Fig. 2). One of

the causes for this discrepancy may be the difference in surface coating. In the study by Farwell et al. (2005), CGNs were cultured on laminin coating, which is capable of inducing actin polymerization through regulation of integrin–laminin interaction, as in the case of astrocytes cultured on laminin (Farwell et al., 1995). Given that integrin $\alpha_V\beta3$ has been identified as a plasma membrane receptor for T4 involved in the regulation of cell proliferation and angiogenesis in cancer cells and endothelial cells (Bergh et al., 2005; Lin et al., 2009), the polylysine coating used in the present study may not be as effective as laminin in recruiting integrin to interact with T4. The fact that rT3 was not effective in promoting CGN survival under our experimental conditions suggests that rT3 may preferentially utilize integrin as its receptor. Another cause of discrepancy between the study by Farwell et al. (2005) and the present study may be the difference in the maturation state of CGNs under the two culture conditions. Judging from the susceptibility to low-K^+-induced cell death, the decrease in TAG-1 expression, and the expression of tau, CGNs examined in the present study were mainly in the postmigratory stage, whereas the cells in the study by Farwell and colleagues were in the premigratory to migratory stage, in which organization of actin plays a major role.

T4, Extracellular K^+, and JNK in the Maturation of Cultured CGNs

By using mouse CGNs, which are viable under the physiological K^+ concentration of 5 mM, it was shown that CGNs in dissociation cultures or organotypic slice cultures undergo temporally regulated development and maturation processes in 5 mM KCl as *in vivo*. In contrast, in 25 mM KCl, CGNs did not reach the final maturation stage unless calcineurin activity was inhibited experimentally (Sato et al., 2005; Okazawa et al., 2009). In K5 + T4, a dramatic reduction was observed in tau phosphorylated at Ser422 between days 2 and 4 of culture, together with a decrease in active JNK (Figs. 5, 6). Ser422 and Ser199 of rat brain tau are highly phosphorylated only during the first 2 weeks of postnatal development, which corresponds to the axon outgrowth and elongation stage (Yu et al., 2009). Phospho-Ser422, in particular, is rapidly dephosphorylated thereafter so that virtually no phosphorylation is observed at this site after 1 month of age. Because microtubule-binding and stabilization activity of tau is negatively regulated by phosphorylation (for review see Mandelkow and Mandelkow, 2012), such developmental phosphorylation of tau is considered a means to ensure a dynamic polymerization–depolymerization cycle of microtubules necessary for axon growth. Phosphorylation followed by dephosphorylation at Ser422 observed in K5 + T4 thus suggests that, under physiological K^+ concentration, T4 induces axonal maturation within 4 days. In contrast, a robust increase of total tau with a sustained level of phosphorylated tau observed in K25 + T4 should result in higher amounts of both phosphorylated and unphosphorylated tau and continuation of axon elongation.

In conclusion, the present study demonstrates novel actions of T4 on cell survival as well as on the neurites of CGNs in culture. T4 induced microtubule polymerization in CGN neurites through distinct mechanisms in K5 and K25. In K5, T4 reduced tau phosphorylation through a decrease in active JNK. In K25, in contrast, T4 increased tau synthesis without reducing the phosphorylation of tau, which may result in active axon growth. Further investigations on how T4 affects the level and the localization of active JNK in differentiating CGNs should provide valuable insights into the importance of TH action in cerebellar development.

ACKNOWLEDGMENTS

The authors have no conflicts of interest.

REFERENCES

Anderson GW. 2008. Thyroid hormone and cerebellar development. Cerebellum 7:60–74.

Bazán-Peregrino M, Gutiérrez-Kobeh L, Morán J. 2007. Role of brain-derived neurotrophic factor in the protective action of N-methyl-D-aspartate in the apoptotic death of cerebellar granule neurons induced by low potassium. J Neurosci Res 85:332–341.

Bergh JJ, Lin HY, Lansing L, Mohamed SN, Davis FB, Mousa S, Davis PJ. 2005. Integrin alphaVbeta3 contains a cell surface receptor site for thyroid hormone that is linked to activation of mitogen-activated protein kinase and induction of angiogenesis. Endocrinology 146:2864–2871.

Bernal J, Nunez J. 1995. Thyroid hormones and brain development. Eur J Endocrinol 133:390–398.

Bernal J. 2002. Action of thyroid hormone in brain. J Endocrinol Invest 25:268–288.

Chang L, Jones Y, Ellisman MH, Goldstein LS, Karin M. 2003. JNK1 is required for maintenance of neuronal microtubules and controls phosphorylation of microtubule-associated proteins. Dev Cell 4:521–533.

Chatonnet F, Guyot R, Picou F, Bondesson M, Flamant F. 2012. Genome-wide search reveals the existence of a limited number of thyroid hormone receptor alpha target genes in cerebellar neurons. PLoS One 7:e30703.

Cheng SY, Leonard JL, Davis PJ. 2010. Molecular aspects of thyroid hormone actions. Endocr Rev 31:139–170.

Coffey ET, Hongisto V, Dickens M, Davis RJ, Courtney MJ. 2000. Dual roles for c-Jun N-terminal kinase in developmental and stress responses in cerebellar granule neurons. J Neurosci 20:7602–7613.

Coffey ET, Smiciene G, Hongisto V, Cao J, Brecht S, Herdegen T, Courtney MJ. 2002. c-Jun N-terminal protein kinase (JNK) 2/3 is specifically activated by stress, mediating c-Jun activation in the presence of constitutive JNK1 activity in cerebellar neurons. J Neurosci 22: 4335–4345.

Davis PJ, Leonard JL, Davis FB. 2008. Mechanisms of nongenomic actions of thyroid hormone. Front Neuroendocrinol 29:211–218.

D'Mello SR, Borodezt K, Soltoff SP. 1997. Insulin-like growth factor and potassium depolarization maintain neuronal survival by distinct pathways: possible involvement of PI 3-kinase in IGF-1 signaling. J Neurosci 17:1548–1560.

Farwell AP, Tranter MP, Leonard JL. 1995. Thyroxine-dependent regulation of integrin–laminin interactions in astrocytes. Endocrinology 136: 3909–3915.

Farwell AP, Dubord-Tomasetti SA, Pietrzykowski AZ, Stachelek SJ, Leonard JL. 2005. Regulation of cerebellar neuronal migration and

neurite outgrowth by thyroxine and 3,3′,5′-triiodothyronine. Brain Res Dev Brain Res 154:121–135.

Farwell AP, Dubord-Tomasetti SA, Pietrzykowski AZ, Leonard JL. 2006. Dynamic nongenomic actions of thyroid hormone in the developing brain. Endocrinology 147:2567–2574.

Gallo V, Kingsbury A, Balázs R, Jorgensen OS. 1987. The role of depolarization in the survival and differentiation of cerebellar granule cells in culture. J Neurosci 7:2203–7213.

Hirai S, Cui de F, Miyata T, Ogawa M, Kiyonari H, Suda Y, Aizawa S, Banba Y, Ohno S. 2006. The c-Jun N-terminal kinase activator dual leucine zipper kinase regulates axon growth and neuronal migration in the developing cerebral cortex. J Neurosci 26:11992–12002.

Hirai S, Banba Y, Satake T, Ohno S. 2011. Axon formation in neocortical neurons depends on stage-specific regulation of microtubule stability by the dual leucine zipper kinase–c-jun N-terminal kinase pathway. J Neurosci 31:6468–6480.

Kimura-Kuroda J, Nagata I, Negishi-Kato M, Kuroda Y. 2002. Thyroid hormone-dependent development of mouse cerebellar Purkinje cells in vitro. Brain Res Dev Brain Res 137:55–65.

Koibuchi N. 2008. The role of thyroid hormone on cerebellar development. Cerebellum 7:530–533.

Koibuchi N, Chin WW. 2000. Thyroid hormone action and brain development. Trends Endocrinol Metab 11:123–128.

Koibuchi N, Jingu H, Iwasaki T, Chin WW. 2003. Current perspectives on the role of thyroid hormone in growth and development of cerebellum. Cerebellum 2:279–289.

Kyriakis JM, Avruch J. 2012. Mammalian MAPK signal transduction pathways activated by stress and inflammation: a 10-year update. Physiol Rev 92:689–737.

Lin HY, Sun M, Tang HY, Lin C, Luidens MK, Mousa SA, Incerpi S, Drusano GL, Davis FB, Davis PJ. 2009. L-thyroxine vs. 3,5,3′-triiodo-L-thyronine and cell proliferation: activation of mitogen-activated protein kinase and phosphatidylinositol 3-kinase. Am J Physiol Cell Physiol 296:C980–C991.

Mandelkow EM, Mandelkow E. 2012. Biochemistry and cell biology of tau protein in neurofibrillary degeneration. Cold Spring Harbor Perspect Med 2:a006247.

Negishi T, Kawasaki K, Sekiguchi S, Ishii Y, Kyuwa S, Kuroda Y, Yoshikawa Y. 2005. Attention-deficit and hyperactive neurobehavioural characteristics induced by perinatal hypothyroidism in rats. Behav Brain Res 159:323V331.

Okazawa M, Abe H, Katsukawa M, Iijima K, Kiwada T, Nakanishi S. 2009. Role of calcineurin signaling in membrane potential-regulated maturation of cerebellar granule cells. J Neurosci 29:2938–2947.

Oliva AA Jr, Atkins CM, Copenagle L, Banker GA. 2006. Activated c-Jun N-terminal kinase is required for axon formation. J Neurosci 26: 9462–4970.

Oppenheimer JH, Schwartz HL. 1997. Molecular basis of thyroid hormone-dependent brain development. Endocr Rev 18:462–475.

Porterfield SP, Hendrich CE. 1993. The role of thyroid hormones in prenatal and neonatal neurological development: current perspectives. Endocr Rev 14:94–106.

Qu C, Li W, Shao Q, Dwyer T, Huang H, Yang T, Liu G. 2013. c-Jun N-terminal kinase 1 (JNK1) is required for coordination of netrin signaling in axon guidance. J Biol Chem 288:1883–1895.

Quignodon L, Grijota-Martinez C, Compe E, Guyot R, Allioli N, Laperrière D, Walker R, Meltzer P, Mader S, Samarut J, Flamant F. 2007. A combined approach identifies a limited number of new thyroid hormone target genes in postnatal mouse cerebellum. J Mol Endocrinol 39:17–28.

Sato M, Suzuki K, Yamazaki H, Nakanishi S. 2005. A pivotal role of calcineurin signaling in development and maturation of postnatal cerebellar granule cells. Proc Natl Acad Sci U S A 102:5874–5879.

Siegrist-Kaiser CA, Juge-Aubry C, Tranter MP, Ekenbarger DM, Leonard JL. 1990. Thyroxine-dependent modulation of actin polymerization in cultured astrocytes. A novel, extranuclear action of thyroid hormone. J Biol Chem 265:5296–5302.

Song B, Lai B, Zheng Z, Zhang Y, Luo J, Wang C, Chen Y, Woodgett JR, Li M. 2010. Inhibitory phosphorylation of GSK-3 by CaMKII couples depolarization to neuronal survival. J Biol Chem 285:41122–1134.

Swiech L, Merycz M, Malik A, Jaworski J. 2008. Role of mTOR in physiology and pathology of the nervous system. Biochim Biophys Acta 1784:116–132.

Takahashi M, Negishi T, Tashiro T. 2008. Identification of genes mediating thyroid hormone action in the developing mouse cerebellum. J Neurochem 104:640–652.

Takemura R, Kanai Y, Hirokawa N. 1991. In situ localization of tau mRNA in developing rat brain. Neuroscience 44:393–407.

Tang Z, Bereczki E, Zhang H, Wang S, Li C, Ji X, Branca RM, Lehtio J, Guan Z, Filipcik P, Xu S, Winblad B, Pei J-J. 2013. Mammalian target of rapamycin (mTOR) mediates tau protein dyshomeostasis. Implication for Alzheimer's disease. J Biol Chem 288:15556–15570.

Thompson CC, Potter GB. 2000. Thyroid hormone action in neural development. Cereb Cortex 10:939–945.

Westerholz S, de Lima AD, Voigt T. 2013. Thyroid hormone-dependent development of early cortical networks: temporal specificity and the contribution of trkB and mTOR pathways. Front Cell Neurosci 7:121.

Williams GR. 2008. Neurodevelopmental and neurophysiological actions of thyroid hormone. J Neuroendocrinol 20:784–794.

Yamagishi S, Yamada M, Ishikawa Y, Matsumoto T, Ikeuchi T, Hatanaka H. 2001. p38 Mitogen-activated protein kinase regulates low potassium-induced c-Jun phosphorylation and apoptosis in cultured cerebellar granule neurons. J Biol Chem 276:5129–5133.

Yamagishi S, Matsumoto T, Yokomaku D, Hatanaka H, Shimoke K, Yamada M, Ikeuchi T. 2003a. Comparison of inhibitory effects of brain-derived neurotrophic factor and insulin-like growth factor on low potassium-induced apoptosis and activation of p38 MAPK and c-Jun in cultured cerebellar granule neurons. Brain Res Mol Brain Res 119: 184–191.

Yamagishi S, Yamada M, Koshimizu H, Takai S, Hatanaka H, Takeda K, Ichijo H, Shimoke K, Ikeuchi T. 2003b. Apoptosis-signal regulating kinase-1 is involved in the low potassium-induced activation of p38 mitogen-activated protein kinase and c-Jun in cultured cerebellar granule neurons. J Biochem 133:719–724.

Yu Y, Run X, Liang Z, Li Y, Liu F, Liu Y, Iqbal K, Grundke-Iqbal I, Gong CX. 2009. Developmental regulation of tau phosphorylation, tau kinases, and tau phosphatases. J Neurochem 108:1480–1494.

Zhang FX, Rubin R, Rooney TA. 1998. N-methyl-D-aspartate inhibits apoptosis through activation of phosphatidylinositol 3-kinase in cerebellar granule neurons. A role for insulin receptor substrate-1 in the neurotrophic action of N-methyl-D-aspartate and its inhibition by ethanol. J Biol Chem 273:26596–26602.

Zhong J, Deng J, Huang S, Yang X, Lee WH. 2004. High K^+ and IGF-1 protect cerebellar granule neurons via distinct signaling pathways. J Neurosci Res 75:794–806.

ELSEVIER

Brain & Development 37 (2015) 88–93

BRAIN & DEVELOPMENT
Official Journal of the Japanese Society of Child Neurology

www.elsevier.com/locate/braindev

Original article

Maternal viral infection during pregnancy impairs development of fetal serotonergic neurons

Takeshi Ohkawara [a,*], Takashi Katsuyama [a], Michiru Ida-Eto [a], Naoko Narita [b], Masaaki Narita [a]

[a] *Department of Developmental and Regenerative Medicine, Mie University, Graduate School of Medicine, Mie, Japan*
[b] *Department of Education, Bunkyo University, Saitama, Japan*

Received 24 October 2013; received in revised form 12 March 2014; accepted 12 March 2014

Abstract

Background: Maternal viral infection during pregnancy induces morphological abnormalities in the fetus and may cause emotional and psychological problems in offspring through unknown mechanisms. We have previously shown that prenatal exposure of rats to chemicals such as thalidomide causes an autistic-like phenotype in offspring, indicating that prenatal events affecting serotonergic development may cause developmental disorder. *Methods:* We investigated whether prenatal viral infection altered the expression of neurotransmitters involved in the emotional or psychological status of offspring. We here took advantage of the polyriboinosinic:polyribocytidylic acid (poly I:C) system, the synthetic double-stranded RNA, which is often used in animal models of viral infection. *Results:* Ten mg/kg of poly I:C was intraperitoneally injected on gestational day (GD) 9 and counted the numbers of serotonin-immunopositive cells on GD15 using flat whole-mount preparation method, resulting 11.1% of increase in the number of serotonergic neurons in poly I:C group. Furthermore, there was a significant decrease in hippocampal serotonin content in offspring by postnatal day 50 following poly I:C administration by high-performance liquid chromatography. *Discussion and Conclusion:* Since serotonin is known to link with behavior and emotion after birth, these results suggest that maternal viral infection might cause, in addition to morphological abnormalities, serotonin-related pathogenesis such as neurodevelopmental disorders including autism spectrum disorders.

Keywords: Maternal viral infection; Autism; Poly I:C; Serotonin

1. Introduction

Maternal viral infection during pregnancy induces morphological abnormalities in the fetus [1,2]. For example, congenital rubella syndrome caused by rubella virus infection during pregnancy, induces fetal cataracts, cardiac defects, and deafness [3]. Cytomegalovirus infection during pregnancy induces intrauterine growth retardation, microphthalmia, microcephalia, and cerebral calcification [4]. In addition to morphological abnormalities, maternal infection may also induce emotional problems in offspring such as schizophrenia [5,6] and mental retardation [7]. However, the mechanisms responsible for these disorders are unknown.

Autism spectrum disorders (ASD) are neurodevelopmental disorder including cognitive and emotional problems [8,9]. The etiologies of ASD are unknown; however, several lines of evidence suggest that disturbances in the embryonic development of serotonergic

* Corresponding author. Address: Mie University, Graduate School of Medicine, 2-174, Edobashi, Tsu, Mie 514-8507, Japan. Tel.: +81 59 232 1111x6326; fax: +81 59 232 8031.
E-mail address: tohkawara@doc.medic.mie-u.ac.jp (T. Ohkawara).

http://dx.doi.org/10.1016/j.braindev.2014.03.007

neurons may be the cause [10–12]. We have shown that embryonic disturbance of serotonergic development induced by thalidomide or valproic acid may cause an autistic phenotype in the offspring of treated rats [13,14] as well as by viral infection.

Serotonin (5-hydroxytryptamine, 5-HT) is a monoaminergic neurotransmitter involved in emotional and mood control [13,15]. Clusters of serotonergic neurons are located in the raphe nuclei of the brainstem. Rostral raphe nuclei start to express the serotonergic neuron phenotype on approximately gestational day (GD) 12 [16]. Ascending serotonergic neurons are first observed on the same day as rostral raphe nuclei, and then they promptly develop diverse axonal projection networks throughout the brain until birth [17].

In the present study, we investigated whether prenatal viral infection changes the serotonergic system. We took advantage of the polyriboinosinic:polyribocytidylic acid (poly I:C) system, which is often used as an animal model of viral infection [18–20].

2. Materials and methods

2.1. Administration of poly I:C

Pregnant Wistar rats were obtained from CLEA Japan, Inc. (CLEA Japan, Inc., Japan). All animal experiments were approved by the Committee of Laboratory Animal Research Center at Mie University. Ten mg/kg of poly I:C (Sigma Aldrich, MO), which is dissolved in sterile phosphate-buffered saline (PBS), or sterile PBS alone was intrapenitorially (i.p.) injected to GD 9 or 10 pregnant Wistar rats. The dose of poly I:C was determined according to a previous study [21].

2.2. Measurement of monoamines and their metabolites using high-performance liquid chromatography (HPLC)

Measurements of monoamines and their metabolites on postnatal (P) day 50 were performed as described previously [22]. Experiments were performed independently twice, and consistent results were obtained from these two experiments. Statistical evaluation was performed using independent Student's t tests. Statistical significance was defined as $p < 0.05$ (two-tailed).

2.3. Flat whole-mount preparation of rat brain and determination of the number of serotonin-immunopositive cells

Flat whole-mount of hindbrains on GD15 was prepared as described previously [23]. GD9 pregnant rats were i.p. injected with poly I:C, and the GD15 fetuses were surgically removed. The embryonic brains were cut along the dorsal midline, opened, and whole-mounted flat with the ventricular side down. The flat, whole-mounted brain was fixed with 4% paraformaldehyde (PFA) overnight at 4 °C and probed with an anti-serotonin antibody as described previously [23]. The numbers of all serotonin-immunopositive cells localized in rostral and caudal clusters were blindly counted to exclude the possibility of bias.

2.4. Quantitative analysis of gene expression during the development of serotonergic neurons

Cranial regions of GD12 embryos were exactly cut just posterior to the forth ventricle, and five embryos were collected from four of each of the pregnant mothers in the two groups. Total RNAs were prepared using TRIzol Reagent (Invitrogen, CA) according to the manufacturer's instructions. One microgram of each total RNA preparation was reverse-transcribed using QuantiTect Reverse Transcription Kit (QIAGEN, Germany) according to the manufacturer's instruction. Real-time PCR reactions using Power SYBR Green PCR Master Mix (Applied Biosystems, CA) were performed using a StepOne Real-Time PCR System (Applied Biosystems, CA). Data were analyzed using the comparative cycle threshold method. *Gapdh* was used as an internal control. Oligonucleotide sequence used for real-time PCR were as follows: *sonic hedgehog* (*Shh*) forward primer:5′-AGCTTCGAGTGACTG AGGGC-3′*Shh* reverse primer: 5′-GTCCCTGTCAG ACGTGGTGA-3′, *fibroblast growth factor 8* (*Fgf8*) forward primer: 5′-CGCAAAGCTCATTGTGGAGA-3′, *Fgf8* reverse primer: 5′-ACACGCAGTCCTTGCCT TTG-3′, *Gata2* forward primer: 5′-AGCCTTGTGCC GCCATTAC-3′, *Gata2* reverse primer: 5′-ACCTGTC CATTTTGCTCTCCA-3′, *Pet-1* forward primer: 5′-TC CCACGACCTACTCAAAC-3′, *Pet-1* reverse primer: 5′-AGGGATGGACAACAGCAGAG-3′, *Gapdh* forward primer: 5′-CAAGTTCAACGGCACAGTCAA G-3′, *Gapdh* reverse primer: 5′-ACATACTCAGCACC AGCATCAC-3′.

2.5. Whole-mount in situ hybridization

Eight embryos from three mothers were used for each group. Whole-mount *in situ* hybridization of GD12 embryos using digoxigenin-labeled complementary RNA (cRNA) probes was performed following Wilkinson's method [24]. In brief, dissected embryos were fixed with 4% PFA in PBS overnight at 4 °C; PFA was removed with a graded-concentration ethanol series, and the samples were stored at −20 °C. Samples were gradually rehydrated and immersed in 0.1% Tween 20 (Sigma–Aldrich) in PBS (PBST). Next, samples were treated with 10 μg/ml proteinase K (Roche Applied Science, IN) for 30 min at 37 °C, fixed again in 0.2% glutaraldehyde, 4% PFA in PBS for 20 min. After two washes with PBST, samples were prehybridized for one hour at

70 °C and hybridized with a digoxigenin-labeled cRNA probe for 16 h at 70 °C. The composition of the hybridization solution was as follows: 50% formamide (WAKO chemicals, Japan), 5 × SSC (pH 7.0), 1% SDS, 50 μg /ml yeast tRNA (Roche Applied Science, IN), and 50 μg/ml heparin sodium salt (Sigma–Aldrich, MO). After hybridization, samples were washed once with 50% formamide, 5 × SSC (pH 4.5); three times with 1% SDS at 70 °C for 30 min; and then three times with 50% formamide and 2 × SSC (pH 4.5) at 65 °C for 30 min. Samples were washed with 25 mM Tris–HCl (pH 7.5), 137 mM NaCl, 2.7 mM KCl, and 0.1% Tween 20 (KTBT) at room temperature (RT). After blocking with 1% blocking reagent (Roche Applied Science, IN) in KTBT for two hours at RT, samples were incubated with Anti-Digoxigenin-AP Fab fragments (Roche Applied Science, IN, 1:2500 dilutions) at RT, and the reactions were detected using 4-nitroblue tetrazolium chloride and 5-bromo-4-chloro-3-indolyl-phosphate. Images were acquired using a KEYENCE VH-5500 microscope system (KEYENCE, Japan). The templates used for probe preparation were as follows: rat *Shh* (2052–3331; GenBank Accession No. AF030355) and rat *Fgf8* (34–560; GenBank Accession No. AB079113).

3. Results

To determine whether prenatal viral infection induces abnormalities in the monoamine systems, we used poly I:C, a double-stranded RNA, which mimics viral infection [18–20] and is therefore frequently used as a model of viral infection. Poly I:C was administered to GD10 pregnant rats because this time window is critical for the early development of serotonergic neurons [13,14,25]. A significant decrease in hippocampal 5-HT levels in the progeny on day P50 was observed in the poly I:C group (control; 196.6 ± 40.2 ng/g weight, poly I:C; 109.3 ± 51.7 ng/g weight, $p < 0.01$) (Table 1). Dopamine (DA) and its metabolites were not detected in the hippocampus. The levels of striatal 5-HT, DA, and their metabolites did not differ between the two groups. These results indicate that prenatal poly I:C administered on GD10 affected 5-HT levels in the hippocampus of the adult brain.

To determine whether decreased hippocampal 5-HT levels in adult progeny of the poly I:C group were caused by abnormal embryonic development of serotonergic neurons, profiles of early serotonergic development were evaluated using the so-called flat whole-mount preparation method. This method facilitates morphological examination during the early embryonic stage of serotonergic neurons developing spatiotemporally in the fetal brain [23,25,26]. Poly I:C or PBS were administered on GD9, embryos were harvested on GD15, and flat whole-mount hindbrain sections were prepared. Fig. 1A shows the two major clusters of serotonergic neurons, which are rostral and caudal cluster [16]. Differences in the basic structure of the raphe between the poly I:C and control groups were not noted initially. Although the number of serotonergic neurons in the caudal cluster did not differ between the two groups (control; 634.8 ± 57.2 cells, poly I:C; 620.3 ± 54.5 cells), close observation revealed that the numbers in the rostral cluster significantly increased in the poly I:C group compared with the control group (Fig. 1B) (control; 276.6 ± 29.1 cells, poly I:C; 307.4 ± 26.9 cells, $p < 0.01$). These results suggest that poly I:C administration during pregnancy perturbs, in part, the early development of serotonergic neurons.

Table 1
Monoamine levels in control ($n = 8$) vs poly I:C injected rats ($n = 5$) on P50.

Monoamines ng/g weight	Group	Hippocampus	Striatum
5-HT	control	196.6 ± 40.2	133.8 ± 34.9
	poly I:C	109.3 ± 51.7*	139.7 ± 47.6
5-HIAA	control	307.2 ± 24.5	273.0 ± 46.1
	poly I:C	314.8 ± 39.6	241.6 ± 77.9
DA	control	N.D.	1295.3 ± 391.3
	poly I:C	N.D.	1147.1 ± 596.2
DOPAC	control	N.D.	802.8 ± 88.9
	poly I:C	N.D.	855.4 ± 142.8
HVA	control	N.D.	345.4 ± 49.3
	poly I:C	N.D.	338.6 ± 58.1

Ten milligrams per kilograms of poly I:C were administered to GD10 rats. On P50, concentrations of hippocampal and striatal monoamines and their metabolites in offspring were measured by HPLC. Consistent results were obtained from independent experiment. Values represent the mean ± standard deviation (SD). N.D.: not detected.*$p < 0.01$ vs. control.

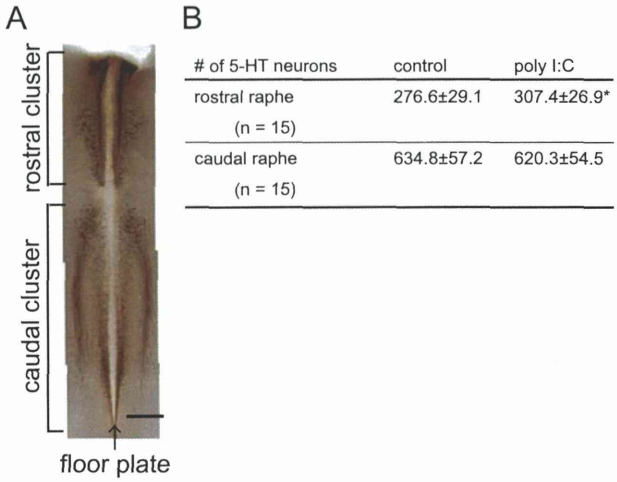

Fig. 1. Effect of poly I:C administration on serotonergic neurons in GD15 rat using flat whole-mount preparations. (A) Low magnification view of the GD15 control stained with anti-serotonin antibody. (B) Comparison of the numbers of serotonin-immunopositive cells in rostral and caudal clusters between the control and poly I:C groups. Numbers represent the average of each determination ± SD. Scale bar represents 500 μm. *$p < 0.01$ vs. control.